

Magnetic properties of the finite-length biatomic chains in the framework of the single domain-wall approximation

S. V. Kolesnikov ^{*}*Faculty of Physics, Lomonosov Moscow State University, Moscow 119991, Russian Federation*

I. N. Kolesnikova

Department of Chemistry, Lomonosov Moscow State University, Moscow 119991, Russian Federation

(Received 5 August 2019; revised manuscript received 8 November 2019; published 26 December 2019)

A simple analytical method for the investigation of the magnetic properties of the finite-length biatomic chains proposed in the framework of the Heisenberg model with uniaxial magnetic anisotropy. The method allows to estimate the reversal time of magnetization of ferromagnetic and antiferromagnetic biatomic chains. Three cases have been considered: the spontaneous remagnetization, the remagnetization under the interaction with a scanning tunneling microscope, and the remagnetization under the external magnetic field. The applicability limits of the method have been discussed. Within its limits of applicability the method produces the results which are in a perfect agreement with those obtained with the use of the kinetic Monte Carlo simulations. As the examples, two physical systems have been considered: biatomic Fe chains on $\text{Cu}_2\text{N}/\text{Cu}(001)$ surface and biatomic Co chains on $\text{Pt}(997)$ surface. The presented method is incomparably less time-consuming than the commonly used kinetic Monte Carlo simulations, especially in the cases of low temperatures or long chains.

DOI: [10.1103/PhysRevB.100.224424](https://doi.org/10.1103/PhysRevB.100.224424)

I. INTRODUCTION

The investigations of the magnetic properties of the atomic chains are of general interest due to its possible applications in spintronics [1], quantum communications [2–4], quantum computing [5], and other fields [6] of research. In particular, atomic chains can be used for the creation of the next generation mass storage devices [7–9]. For application of the atomic chains as bits of information, their reversal time of magnetization needs to be sufficiently long. The possibility of engineering of such memory elements [10] appeared after the discovery of the giant magnetic anisotropy energy (MAE) of Co atoms on the $\text{Pt}(997)$ surface [11,12] using x-ray magnetic circular dichroism and scanning tunneling microscope (STM) [13–15]. Ferromagnetic Co chains can grow on the step edges of $\text{Pt}(997)$ surface at low concentrations of Co atoms. The analogous effect was observed for $\text{Fe}/\text{Cu}(111)$ system [16,17]. The critical temperature T_C and the reversal time of magnetization τ of the atomic chains increase with their length. According to the estimation [12] the atomic chain consisting of 400 Co atoms can be a stable bit of information at room temperature. In order to increase the information recording density, it is possible to use biatomic ferromagnetic chains [18,19]. However, an increase of the chain width usually leads to the significant decrease of MAE [19–21]. These observations are in a good agreement with a well-known effect of decreasing of the average MAE of atoms in atomic clusters with an increase of their size [22–24].

Another interesting opportunity is use of finite-sized antiferromagnetic chains as bits of information [25–28]. The

interaction between antiferromagnetic chains is much weaker than between ferromagnetic ones. Therefore, the use of antiferromagnetic chains can lead to a significant increase in the information recording density. The possibility of creating and remagnetization of such chains using STM was demonstrated for Fe atomic chains on $\text{Cu}_2\text{N}/\text{Cu}(001)$ surface [29,30]. A systematic study of atomic chains composed of the transition metals on $\text{Cu}_2\text{N}/\text{Cu}(001)$ surface has shown that they can be either ferromagnetic or antiferromagnetic [31–35]. Very similar results are obtained for the analogous atomic chains on $\text{Cu}_2\text{O}/\text{Cu}(001)$ surface [36]. Biatomic antiferromagnetic chains are known to be significantly more stable than the single-atomic chains [30]. A special attention should be paid to the investigations of the remagnetization of the atomic chains with the STM tip. It has been shown that the switching of magnetization at high STM voltages is mediated by domain-wall formation and propagation [37].

A lot of theoretical investigations have been devoted to ferromagnetic and antiferromagnetic finite-sized chains. Among them it is necessary to underline the studies devoted to the influence of quantum tunneling on the reversal time of magnetization [37–39]. Quantum tunneling is the main switching mechanism at extremely low temperatures below the mK range for a system consisting of six Fe atoms [38]. However, we can neglect the quantum nature of the atomic magnetic moments at higher temperatures. In this case the magnetic properties of atomic chains can be described in the framework of the classical Heisenberg Hamiltonian and its generalizations.

The parameters of the Heisenberg Hamiltonian can be calculated from the first principles by the means of density functional theory [18,36,40] or Korringa-Kohn-Rostoker-Green's function method [15,41]. Further investigation of the

*kolesnikov@physics.msu.ru

magnetic properties of atomic chains can be performed with either the solution of the Landau–Lifshitz–Gilbert equation [40,42] or the kinetic Monte Carlo (kMC) simulations [43]. The kMC method allows to calculate the critical temperature, the reversal time of magnetization, and the coercive field of ferromagnetic chains [44–48]. The process of dynamical magnetization of rectangular lattices composed of tiny magnets with strong perpendicular uniaxial anisotropy also studied [49]. It was shown that the kMC method can be successfully applied for the investigation of antiferromagnetic chains as well [50,51].

However, the kMC method is a statistical method and the process of obtaining of the averaged values with small errors always needs a lot of simulations. Commonly used kMC simulations can be very time-consuming, especially in the cases of low temperatures or long chains. Thus, it would be useful to find a simple analytical method to estimate the reversal time of magnetization, which would be in a good agreement with the results of the kMC simulations in a wide range of parameters. Such method in the single domain-wall approximation was developed earlier for the single-atomic chains [52,53]. It was shown that the single domain-wall approximation is justified in a wide range of parameters of the Heisenberg Hamiltonian and a wide range of temperatures. The proposed method allows to estimate the reversal time of magnetization of ferromagnetic chains in the cases of a spontaneous remagnetization and the remagnetization under the external magnetic field [52]. The reversal time of magnetization of antiferromagnetic chains under the interaction with the STM tip also can be correctly estimated [53].

In this article, the previously developed formalism [52,53] is generalized to the case of biatomic chains [54]. Two limiting cases will be considered: a weak and a strong coupling between the atomic chains. It will be shown that these two approximations cover a wide range of parameters and can be used in a lot of practically interesting situations. The estimation formulas for the reversal time of magnetization of biatomic chains will be derived in the three following cases of remagnetization: (i) spontaneous, (ii) under the interaction with STM tip, and (iii) under the external magnetic field. It will be shown that the proposed method allows to calculate the magnetization curves and the coercive fields of biatomic ferromagnetic chains. The obtained analytical results will be compared with the results obtained with the use of the kMC simulations.

The paper is organized as follows. In Sec. II, the theoretical model is briefly discussed. In Sec. III A, the estimation formulas for the reversal time of magnetization in the case of spontaneous remagnetization of both ferromagnetic and antiferromagnetic biatomic chains are derived. Interaction of biatomic chains with STM is discussed in Sec. III B. Remagnetization of ferromagnetic biatomic chains under the external magnetic field is investigated in Sec. III C. In order to demonstrate the ability of the method to estimate the reversal time of magnetization some numerical results are compared with the results of the kMC simulations in Sec. III D. The conclusions are presented in Sec. IV. For the reader's convenience, the main results from Refs. [52,53] are summarized in Appendix A. The estimation of thickness of a domain wall is presented in Appendix B.

II. THEORETICAL MODEL

In order to estimate the reversal time of magnetization we assume that we can neglect quantum tunneling at the temperatures $T > T_{QT}$ and consider the magnetic moments of atoms as classical vectors. Temperature T_{QT} has an order of mK for the chains under consideration [38]. Following the paper of Li and Liu [43] we consider the case of uniaxial magnetic anisotropy. Thus, the Heisenberg Hamiltonian can be written in the following form

$$H = - \sum_{i>j} J_{ij}(\mathbf{s}_i \cdot \mathbf{s}_j) - K \sum_i (\mathbf{s}_i \cdot \mathbf{e})^2 - \mu \sum_i (\mathbf{s}_i \cdot \mathbf{B}), \quad (1)$$

where \mathbf{s}_i and \mathbf{e} are the unit vectors of the magnetic moments of atoms and the easy axis of magnetization, respectively, μ is the absolute value of magnetic moments, K is MAE, $J_{ij} = J(\delta_{i,j+1} + \delta_{i,j-1})$ is the exchange energy, and δ_{ij} is Kronecker δ . For ferromagnetic chains $J > 0$ and for antiferromagnetic chains $J < 0$. The external magnetic field \mathbf{B} is assumed to be applied along the easy axis of magnetization \mathbf{e} . We assume that all of the magnetic moments are directed either parallel or antiparallel to the easy axis of magnetization $(\mathbf{s}_i \cdot \mathbf{e}) = \pm 1$. We can say that the magnetic moment is directed “up” if $(\mathbf{s}_i \cdot \mathbf{e}) = 1$ and “down” if $(\mathbf{s}_i \cdot \mathbf{e}) = -1$.

The flipping of the i th magnetic moment can occur in two different ways [55]. If $2K > |h_i|$ [where $h_i = \sum_j J_{ij}(\mathbf{s}_i \cdot \mathbf{s}_j) + \mu(\mathbf{s}_i \cdot \mathbf{B})$], then the rate of a single magnetic moment flip is determined as [43]

$$\nu(h_i) = \nu_0 \exp \left[- \frac{(2K + h_i)^2}{4Kk_B T} \right], \quad (2)$$

where k_B is the Boltzmann constant, T is the temperature, and ν_0 is the frequency prefactor. If $2K \leq |h_i|$, then there is no energy barrier between the states $(\mathbf{s}_i \cdot \mathbf{e}) = \pm 1$. The rate of a single magnetic moment flip can be calculated [56], as

$$\nu(h_i) = \nu_0 \frac{\exp(-2h_i/k_B T)}{1 + \exp(-2h_i/k_B T)}. \quad (3)$$

Below we will use the function $\nu(h_i)$, which defined by Eqs. (2) and (3) [57]. The frequency prefactor $\nu_0 = 10^9$ Hz [11] is chosen for the numerical estimates.

The main ideas of the proposed method are demonstrated further on the example of a ferromagnetic chain consisting of 10 atoms. Let us assume that all magnetic moments are directed up in the initial moment of time (Fig. 1) and the process of chain remagnetization is associated with the formation and propagation of a single domain wall. If $J/2KN^2 \ll 1$, then the thickness of the domain wall can be neglected (see Appendix B). Dashed lines in Fig. 1 show the possible positions $i = 0, \dots, 10$ of the domain wall. Solid lines show its current position: (a) $i = 0$, (b) $i = 5$, (c) $i = 9$. The domain wall leaves initial state $i = 0$, moves randomly along the chain, and comes to final state $i = 10$. The reversal time of magnetization τ of the atomic chain is defined as the average time of the random walk of the domain wall. If the parameters of the Hamiltonian (1) are the same for all of the atoms and $\mathbf{B} = 0$, then the random walk of the domain wall is characterized by only three rates: (i) the rate of formation of the domain wall ν_1 [Fig. 1(a)], (ii) the rate of the domain wall disappearance ν_2 [Fig. 1(c)], and (iii) the rate of motion of the

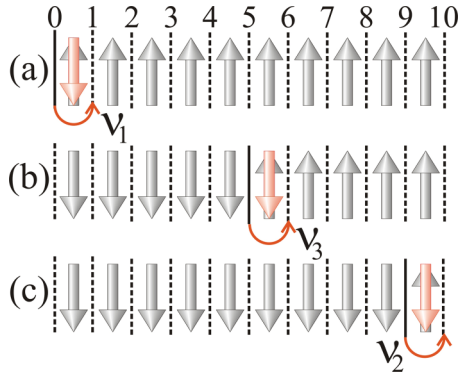


FIG. 1. A schematic view of the atomic chain consisting of $N = 10$ magnetic moments. Dashed lines show the possible positions $i = 0, \dots, 10$ of the domain wall. Solid lines show its current position. The following processes are shown: (a) formation of the domain wall with the rate of v_1 , (b) motion of the domain wall with the rate of v_3 , and (c) the domain wall disappearance with the rate of v_2 . Red arrows show the flipping magnetic moments.

domain wall along the chain v_3 [Fig. 1(b)]. The rate $v_{1,2,3}$ can be easily calculated using Eqs. (2) and (3). We assume that two domain walls are not able to exist simultaneously if the temperature is lower than $T_{\max} < T_C$. Thus, our model is valid in the temperature range of $T_{QT} < T < T_{\max}$.

To calculate the average time of the random walk of the domain wall the mean rate method is employed [58,59]. At the first step the rates $v_{i \rightarrow j}$ of all of the possible transitions of the domain wall should be calculated and the transition probability matrix should be found [60]

$$T_{ij} = \tau_j^1 v_{j \rightarrow i}, \quad (4)$$

where $\tau_j^1 = (\sum_k v_{j \rightarrow k})^{-1}$ is the mean residence time in the state j each time it is occupied, indexes i and j run over initial and all of transient states of the domain wall, index k runs over all possible states (including final states) of the domain wall. The probability P_i to find the domain wall in the state i can be calculated from the following system of linear equations:

$$\sum_{j=0}^{N-1} (\delta_{ij} - T_{ij}) P_j = P_i^{\text{init}}, \quad (5)$$

where $P_i^{\text{init}} = \delta_{0i}$ is the probability to find the domain wall in the state i at the initial moment of time. The average time of the random walk of the domain wall can be obtained as

$$\tau_{\text{tot}} = \sum_{i=0}^{N-1} \tau_i^1 P_i. \quad (6)$$

If the remagnetization of the chain can begin from any of its ends with the same probability, then its reversal time of magnetization τ is equal to $\tau_{\text{tot}}/2$.

III. RESULTS AND DISCUSSIONS

Following the experimental study [30] we consider biatomic chains of two types: type A and type B (see Fig. 2). We assume that the exchange energy J characterizes the interactions between the nearest atoms in the same atomic

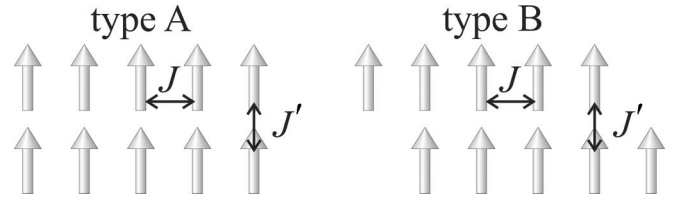


FIG. 2. Two types of the biatomic chains under consideration: (a) type A and (b) type B. Exchange energies J and J' characterize the coupling between the neighboring atoms.

chain, and J' characterizes the interactions between atoms of the neighboring atomic chains. For simplicity, the interactions between other pairs of atoms are neglected. Rates $v(h_i)$ which will be used below can be calculated by means of Eqs. (2) and (3). The following rates will be necessary: $v_1 = v(|J| + |J'|)$, $v'_1 = v(|J| - |J'|)$, $v''_1 = v(|J|)$, $v_2 = v(-|J| + |J'|)$, $v'_2 = v(-|J| - |J'|)$, $v''_2 = v(-|J|)$, $v_3 = v(|J'|)$, $v'_3 = v(-|J'|)$, $v''_3 = v(0)$ if $\mathbf{B} = 0$, and $v_{1\pm} = v(J + J' \pm \mu B)$, $v'_{1\pm} = v(J - J' \pm \mu B)$, $v''_{1\pm} = v(J \pm \mu B)$, $v_{2\pm} = v(-J + J' \pm \mu B)$, $v'_{2\pm} = v(-J - J' \pm \mu B)$, $v''_{2\pm} = v(-J \pm \mu B)$, $v_{3\pm} = v(J' \pm \mu B)$, $v'_{3\pm} = v(-J' \pm \mu B)$, $v''_{3\pm} = v(\pm \mu B)$ if $\mathbf{B} \neq 0$. Below, we derive equations for estimation of the reversal time of magnetization of biatomic chains in two limiting cases: (i) a weak coupling between the atomic chains ($|J'| \ll |J|$) and (ii) a strong coupling between the chains ($|J'| \gtrsim |J|$). The parameters of the Heisenberg Hamiltonian are assumed to be the same for all of the atoms. Edge effects can be taken into account as well as in the case of single-atomic chains (see Ref. [53] and Eqs. (A6) and (A7) in Appendix A).

A. Spontaneous remagnetization

First the case of spontaneous remagnetization of biatomic chains in the absence of external fields (no interaction with the STM tip, no external magnetic field) will be investigated. How it can be seen further, all of the equations for the reversal times of magnetization include the absolute values of the exchange energies $|J|$ and $|J'|$. Thus, all of the results obtained in this section are valid for both ferromagnetic and antiferromagnetic chains.

1. Weak-coupling approximation

Let us consider weakly interacting atomic chains ($|J'| \ll |J|$). This case is directly related to the experimental study [30], because the ratio between the exchange energies of the Fe atoms on $\text{Cu}_2\text{N}/\text{Cu}(001)$ surface is $J/J' \approx 40$. We assume that the atomic chains flip one by one (see Fig. 3). So the atomic chain is flipping at the current moment under the effective magnetic field which is created by another chain. The initial state, two transient states, and the final state of a biatomic chain are denoted as 0, 1, 2, and 3, respectively. Then

$$v_{0 \rightarrow 1} = v_{0 \rightarrow 2} = v_{3 \rightarrow 1} = v_{3 \rightarrow 2} = v_+, \quad (7)$$

$$v_{1 \rightarrow 0} = v_{2 \rightarrow 0} = v_{1 \rightarrow 3} = v_{2 \rightarrow 3} = v_-, \quad (8)$$

$$v_{0 \rightarrow 3} = v_{3 \rightarrow 0} = 0. \quad (9)$$

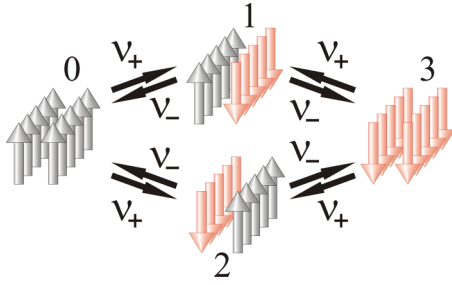


FIG. 3. A schematic view of remagnetization of a biatomic chain in a weak-coupling approximation: 0 is the initial state, 1 and 2 are the transient states, and 3 is the final state. Red arrows represent flipping magnetic moments.

The nonzero elements of the transition probability matrix calculated by Eq. (4) are equal to $T_{0i} = 1/2$, $T_{i0} = 1/2$, where $i = 1, 2$. After solving the system of Eqs. (5) with $P^{\text{init}} = \{1, 0, 0\}$ we find the reversal time of magnetization in the weak-coupling approximation

$$\tau^{\text{weak}} = \tau_+ + \tau_-, \quad (10)$$

where $\tau_+ = 1/\nu_+$ and $\tau_- = 1/\nu_-$.

The reversal times of magnetization τ_+ and τ_- are different for biatomic chains of type A and type B. For the chains of type A, all of the atoms of the second atomic chain are in the effective magnetic field $B = |J'|/\mu$ created by the atoms of the first atomic chain at the transition $0 \rightarrow 1$ (see Fig. 3). Therefore, the reversal time of magnetization of the second atomic chains can be estimated by Eq. (A5) in which the following replacements are made: $\nu''_{1+} \rightarrow \nu_1$, $\nu''_{1-} \rightarrow \nu'_1$, $\nu''_{2+} \rightarrow \nu_2$, $\nu''_{2-} \rightarrow \nu'_2$, $\nu''_{3+} \rightarrow \nu_3$, $\nu''_{3-} \rightarrow \nu'_3$, i.e.,

$$\tau_+ = \tau_B \left(\frac{|J'|}{\mu} \right). \quad (11)$$

All of the atoms of the first atomic chain are under the effective magnetic field $B = -|J'|/\mu$ created by the atoms of the second atomic chain at the transition $1 \rightarrow 3$. Thus,

$$\tau_- = \tau_B \left(-\frac{|J'|}{\mu} \right). \quad (12)$$

Replacing $|J'| \rightarrow -|J'|$ is equivalent to replacing of $\nu_i \rightarrow \nu'_i$, $\nu'_i \rightarrow \nu_i$ in Eq. (11), where $i = 1, 2, 3$.

In the case of the biatomic chain of type B, one of the edge atoms of each atomic chains does not interact with atoms of another chain. In the other words, one of the ends of each atomic chain is “free.” Let us consider the transition $0 \rightarrow 1$. In this case remagnetization depends on the type of the end at which it starts from. If the remagnetization begins at “free” end, then the reversal time of magnetization can be estimated by Eq. (A5) after the replacements $\nu''_{1+} \rightarrow \nu'_1$, $\nu''_{2-} \rightarrow \nu'_2$ and multiplying by a factor of 2:

$$\tau_{1+} = 2\tau_B \left(\frac{|J'|}{\mu}; \nu''_{1+} \rightarrow \nu'_1, \nu''_{2-} \rightarrow \nu'_2 \right). \quad (13)$$

If remagnetization of the second atomic chain begins at another end, then the reversal time of magnetization is the

following:

$$\tau_{2+} = 2\tau_B \left(\frac{|J'|}{\mu}; \nu''_{1-} \rightarrow \nu'_1, \nu''_{2+} \rightarrow \nu'_2 \right). \quad (14)$$

Then the average reversal time of magnetization of the second chain is equal to

$$\tau_+ = \left(\frac{1}{\tau_{1+}} + \frac{1}{\tau_{2+}} \right)^{-1}. \quad (15)$$

The similar result is obtained for the transition $1 \rightarrow 3$:

$$\tau_- = \left(\frac{1}{\tau_{1-}} + \frac{1}{\tau_{2-}} \right)^{-1}, \quad (16)$$

where

$$\tau_{1-} = 2\tau_B \left(-\frac{|J'|}{\mu}; \nu''_{1+} \rightarrow \nu'_1, \nu''_{2-} \rightarrow \nu'_2 \right), \quad (17)$$

$$\tau_{2-} = 2\tau_B \left(-\frac{|J'|}{\mu}; \nu''_{1-} \rightarrow \nu'_1, \nu''_{2+} \rightarrow \nu'_2 \right). \quad (18)$$

Finally, we find the reversal time of magnetization τ^{weak} of the biatomic chains in a weak-coupling approximation by substituting either (11) and (12) for the chains of type A, or (15) and (16) for the chains of type B to Eq. (10). Note that when $|J'| \rightarrow 0$ the value of τ^{weak} tends to $2\tau_1$, where τ_1 is the reversal time of magnetization of a single-atomic chain in the absence of external fields and calculated by Eq. (A1).

2. Strong-coupling approximation

In the case of a strong coupling between the atomic chains ($|J'| \gtrsim |J|$) the length of the domain wall should be minimal. So, the domain wall must be perpendicular to the biatomic chain. First we consider the case of the biatomic chain of type A. The positions of the domain wall corresponding to the local minima of the energy are shown in Fig. 4. To estimate the reversal time of magnetization of a biatomic chain, it is necessary to calculate the rates $\tilde{\nu}_1$, $\tilde{\nu}_2$, $\tilde{\nu}_3$, and $\tilde{\nu}'_3$ of formation, disappearance, and motion of the domain wall, respectively.

Let us calculate the rate of motion of the domain wall $\tilde{\nu}_3$. Figure 5 shows that the domain wall can transit from the initial state 0 to one of the two equivalent final states I or II through the transient states 1, 2, 3, and 4. The nonzero transition rates are equal to

$$\nu_{0 \rightarrow i} = \nu_3, \quad (19)$$

$$\nu_{i \rightarrow 0} = \nu_{1 \rightarrow \text{I}} = \nu_{2 \rightarrow \text{II}} = \nu_{3 \rightarrow \text{I}} = \nu_{4 \rightarrow \text{II}} = \nu'_3, \quad (20)$$

where $i = 1, 2, 3, 4$. The nonzero elements of the transition probability matrix calculated by Eq. (4) are equal to $T_{0i} = 1/2$, $T_{i0} = 1/4$. After solving the system of Eqs. (5) with $P^{\text{init}} = \{1, 0, 0, 0, 0\}$ we find

$$\tilde{\nu}_3 = \frac{\tau_1^1 P_1 \nu_{1 \rightarrow \text{I}} + \tau_3^1 P_3 \nu_{3 \rightarrow \text{I}}}{\tau_{\text{tot}}} = \frac{\nu_3 \nu'_3}{\nu'_3 + 2\nu_3}. \quad (21)$$

To calculate the rate of formation of the domain wall $\tilde{\nu}_1$ similar procedure is used. Figure 6 shows that the domain wall can transit from the initial state 0 to the final state 3 through the transient states 1 or 2. The nonzero transition rates are

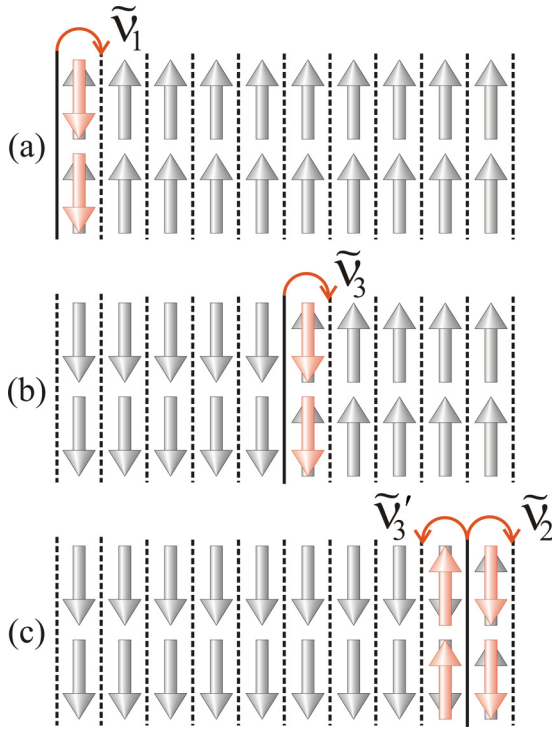


FIG. 4. A schematic view of a biatomic chain of type A consisting of $2N = 20$ magnetic moments. Dashed lines show the stable positions of the domain wall in a strong-coupling approximation. Solid lines show current positions of the domain wall. The following processes are shown: (a) formation of the domain wall with the rate of \tilde{v}_1 , (b) motion of the domain wall with the rate of \tilde{v}_3 , and (c) the domain wall disappearance with the rate of \tilde{v}_2 and motion of the domain wall near the end of the chain with the rate of \tilde{v}'_3 . Red arrows represent the flipping magnetic moments.

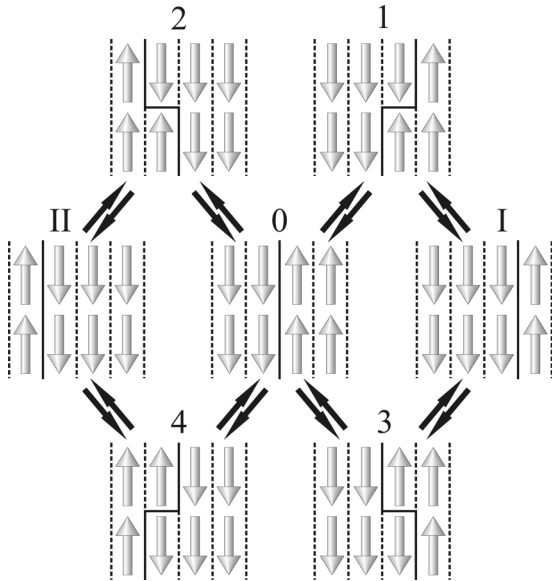


FIG. 5. A schematic view of the domain wall motion in a strong-coupling approximation: 0 is the initial state; 1, 2, 3, and 4 are the transient states; I and II are the final states. Red arrows represent the flipping magnetic moments.

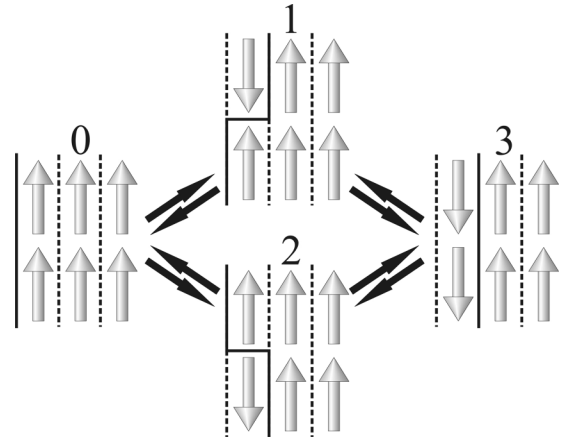


FIG. 6. A schematic view of formation of the domain wall in the chain of type A in a strong-coupling approximation: 0 is the initial state, 1 and 2 are the transient states, and 3 is the final state. Red arrows show the flipping magnetic moments.

equal to

$$v_{0 \rightarrow i} = v_1, \quad v_{i \rightarrow 3} = v'_1, \quad v_{i \rightarrow 0} = v'_2, \quad (22)$$

where $i = 1, 2$. The nonzero elements of the transition probability matrix are equal to $T_{0i} = v'_2/(v'_1 + v'_2)$, $T_{i0} = 1/2$. After solving the system of Eqs. (5) with $P^{\text{init}} = \{1, 0, 0\}$ we find

$$\tilde{v}_1 = \frac{\tau_1^1 P_1 v_{1 \rightarrow 3} + \tau_2^1 P_2 v_{2 \rightarrow 3}}{\tau_{\text{tot}}} = \frac{2v_1 v'_1}{v_1 + v'_1 + v'_2}. \quad (23)$$

Finally, let us calculate the rate of the domain wall disappearance \tilde{v}_2 and the rate \tilde{v}'_3 . The domain wall can transit from the initial state 0 to one of two nonequivalent final states I or II through the transient states 1, 2, 3, and 4 (see Fig. 7). The nonzero transition rates are equal to

$$v_{0 \rightarrow 1} = v_{0 \rightarrow 3} = v_3, \quad v_{0 \rightarrow 2} = v_{0 \rightarrow 4} = v_2, \quad (24)$$

$$v_{1 \rightarrow 0} = v_{3 \rightarrow 0} = v_{1 \rightarrow \text{I}} = v_{3 \rightarrow \text{I}} = v'_3, \quad (25)$$

$$v_{2 \rightarrow 0} = v_{4 \rightarrow 0} = v'_1, \quad v_{2 \rightarrow \text{II}} = v_{4 \rightarrow \text{II}} = v'_2. \quad (26)$$

The nonzero elements of the transition probability matrix are equal to $T_{01} = T_{03} = 1/2$, $T_{02} = T_{04} = v'_1/(v'_1 + v'_2)$, $T_{10} = T_{30} = a/2$, and $T_{20} = T_{40} = (1 - a)/2$, where $a = v_3/(v_2 + v_3)$. After solving the system of Eqs. (5) with $P^{\text{init}} = \{1, 0, 0, 0, 0\}$ we find

$$\begin{aligned} \tilde{v}_2 &= \frac{\tau_2^1 P_2 v_{2 \rightarrow \text{II}} + \tau_4^1 P_4 v_{4 \rightarrow \text{II}}}{\tau_{\text{tot}}} \\ &= \frac{2v_2 v'_2 v'_3}{v_3(v'_1 + v'_2) + v'_3(2v_2 + v'_1 + v'_2)}, \end{aligned} \quad (27)$$

$$\begin{aligned} \tilde{v}'_3 &= \frac{\tau_1^1 P_1 v_{1 \rightarrow \text{I}} + \tau_3^1 P_3 v_{3 \rightarrow \text{I}}}{\tau_{\text{tot}}} \\ &= \frac{v_3 v'_3 (v'_1 + v'_2)}{v_3(v'_1 + v'_2) + v'_3(2v_2 + v'_1 + v'_2)}. \end{aligned} \quad (28)$$

Now the problem of remagnetization of a biatomic chain is reduced to the problem of remagnetization of a single-atomic chain. In order to estimate the reversal time of magnetization

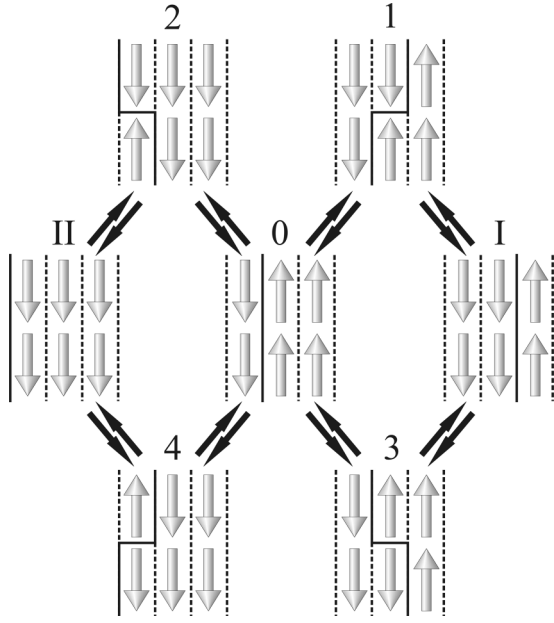


FIG. 7. A schematic view of the domain wall disappearance and motion of the domain wall near the end of a chain of type A in a strong-coupling approximation: 0 is the initial state; 1, 2, 3, and 4 are the transient states; and I and II are the final states, respectively. Red arrows represent the flipping magnetic moments.

τ^{strong} , Eq. (A7) should be used with the following replacements: $v_1'' \rightarrow \tilde{v}_1$, $v_2'' \rightarrow \tilde{v}_2$, $v_2, v_3'' \rightarrow \tilde{v}_3$, $v_1' \rightarrow \tilde{v}_3'$. Then

$$\tau^{\text{strong}} = \frac{1}{2\tilde{a}} \left\{ \frac{\tilde{a}}{2\tilde{v}_3} \left(N - 3 + 2\frac{\tilde{v}_3}{\tilde{v}_3'} \right) \left[N - \frac{2(1-2\tilde{a})}{1-\tilde{a}} \right] + \frac{1}{\tilde{v}_1} [N(1-\tilde{a}) - 2(1-2\tilde{a})] \right\}, \quad (29)$$

where $\tilde{a} = \tilde{v}_3' / (\tilde{v}_2 + \tilde{v}_3')$. This equation has the same structure as Eq. (A1).

Now we consider a spontaneous remagnetization of a biatomic chain of type B. Figure 8 shows the positions of the domain wall corresponding to the local minima of energy. The rate \tilde{v}_3 of the domain wall motion obviously does not depend on the type of a biatomic chain. The value of \tilde{v}_3 is determined by Eq. (21). The calculation of the rates \tilde{v}_1 , \tilde{v}_2 , and \tilde{v}_3' is similar to the case A. Here, only the final equations are presented:

$$\tilde{v}_1 = v_1'' \left[\frac{v_1' v_3}{v_1' + v_3'} + \frac{v_1 v_3'}{v_2' + v_3'} \right] \times \left[v_1 + v_1'' + v_2'' + v_3 + \frac{v_3(v_1' - v_3')}{v_1' + v_3'} + \frac{v_1(v_1'' - v_2')}{v_2' + v_3'} \right]^{-1}, \quad (30)$$

$$\tilde{v}_2 = v_2'' v_3' \frac{v_2' v_3(v_1' + v_3') + v_2 v_3'(v_2' + v_3')}{(v_3 + v_3')F_1 + v_3'F_2}, \quad (31)$$

$$\tilde{v}_3' = \frac{v_3 v_3' F_1}{(v_3 + v_3')F_1 + v_3'F_2}, \quad (32)$$

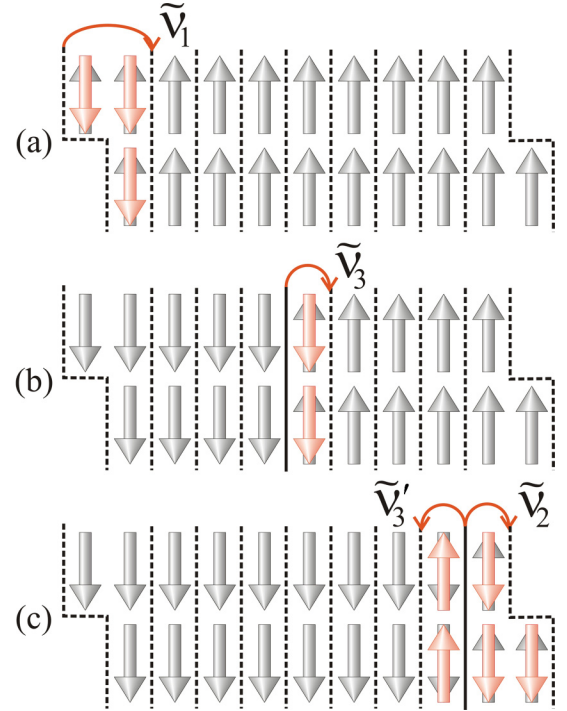


FIG. 8. A schematic view of the biatomic chain of type B consisting of $2N = 20$ magnetic moments. Dashed lines show the stable positions of the domain wall in a strong-coupling approximation. Solid lines show its current position. The following processes are shown: (a) Formation of the domain wall with the rate of \tilde{v}_1 , (b) motion of the domain wall with the rate of \tilde{v}_3 , and (c) the domain wall disappearance with the rate of \tilde{v}_2 and motion of the domain wall near the end of the chain with the rate of \tilde{v}_3' . Red arrows represent the flipping magnetic moments.

where

$$F_1 = (v_1 + v_2'' + v_3)(v_1' + v_3')(v_2' + v_3') - v_3 v_3'(v_2' + v_3') - v_1 v_2'(v_1' + v_3'), \quad (33)$$

$$F_2 = (v_1 + v_2'' + v_3)[v_3(v_1' + v_3') + v_2(v_2' + v_3')] + (v_2' - v_3')(v_3^2 - v_1 v_2) + v_2 v_3(v_1' + v_3') + v_2 v_3'(v_2' + v_3'). \quad (34)$$

To estimate the reversal time of magnetization τ^{strong} we need to substitute the rates (30), (31), and (32) to Eq. (29) and to replacement N by $N - 1$.

B. Interaction with STM

As shown in Ref. [37], the remagnetization of antiferromagnetic chains occurs due to the formation of a domain wall at high voltages between the surface and the STM tip. This regime of remagnetization is considered in the current section. It is assumed that the magnetic moment of the atom located under the STM tip immediately flips and cannot return to its initial state. Then the reversal time of magnetization of a biatomic chain (τ_{STM}) is also the reversal time of magnetization of all other atoms. The STM tip is assumed to be located over the one of the edge atoms of a biatomic chain

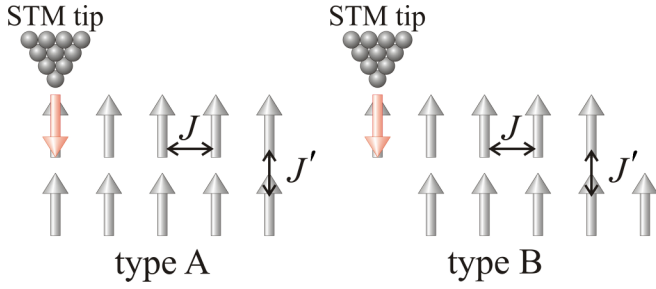


FIG. 9. A schematic view of the interaction between the STM tip and biatomic chains of types A and B. Red arrows represent the magnetic moment which flips as a result of this interaction.

[30]. The location of the STM tip and the magnetic moments of the atoms at the initial moment of time are shown in Fig. 9. A single domain-wall approximation and the assumption that the domain wall is already formed at the initial moment of time near the STM tip are applied. So in the framework of our model the remagnetization of a biatomic chain always begins from one end. Further solution of the problem is different in the cases of a weak and a strong interaction between atomic chains.

1. Weak-coupling approximation

In the case of a weak coupling between atomic chains it is assumed that in the beginning only the first chain which interacts with the STM tip is remagnetized. The remagnetization of the second chain starts only when the remagnetization of the first chain is finished. Therefore, the total reversal time of magnetization is equal to the sum of the reversal times of the magnetization of two atomic chains.

$$\tau_{\text{STM}}^{\text{weak}} = \tau_{+}^{\text{STM}} + \tau_{-}, \quad (35)$$

where the value of τ_{-} is calculated by Eq. (12) or (16), for the chains of type A or B, respectively. The reversal time of magnetization τ_{+}^{STM} does not depend on the type of the chain (see Fig. 9). Its value can be determined by comparing Eqs. (A1), (A2), (A3), and (A5), in which μB should be replaced by $|J'|$:

$$\tau_{+}^{\text{STM}} = \frac{a_{-}}{v'_{3}(1-a_{-})} + \frac{(N-2)(1-a_{-}) + (a_{-}-\alpha)S_{N-2}}{v_{3}(1-\alpha)(1-a_{-})}, \quad (36)$$

where $\alpha = (1-b)/b$, $S_N = (1-\alpha^N)/(1-\alpha)$, $a_{-} = v'_{3}/(v_2 + v'_3)$, and $b = v_3/(v_3 + v'_3)$.

2. Strong-coupling approximation

In the case of a strong interaction between the chains, the calculations similar to those presented in Sec. III A should be performed. The rate of motion of the domain wall along the chain \tilde{v}_3 is still determined by Eq. (21). The rates \tilde{v}_1 , \tilde{v}_2 , and \tilde{v}'_3 for the free end of a biatomic chain are also not changed. The rates \tilde{v}_1^{STM} , \tilde{v}_2^{STM} , and $\tilde{v}'_3^{\text{STM}}$ for the end of the biatomic chain interacting with the STM tip should be calculated. Then Eq. (29) will be generalized to the case of chains with nonequivalent ends.

The calculation of the rates is completely analogous to the one presented above. For chains of type A:

$$\tilde{v}_1^{\text{STM}} = v'_1, \quad (37)$$

$$\tilde{v}_2^{\text{STM}} = \frac{v_2 v'_3}{v_3 + v'_3}, \quad (38)$$

$$\tilde{v}'_3^{\text{STM}} = \frac{v_3 v'_3}{v_3 + v'_3}. \quad (39)$$

For the chains of type B:

$$\tilde{v}_1^{\text{STM}} = \frac{v'_1 v_3 (v'_2 + v'_3) + v_1 v'_3 (v'_1 + v'_3)}{(v'_1 + v'_3)(v'_2 + v'_3) + v_3 (v'_2 + v'_3) + v_1 (v'_1 + v'_3)}, \quad (40)$$

$$\tilde{v}_2^{\text{STM}} = \frac{v'_3}{F_3} [v'_2 v_3 (v'_1 + v'_3) + v_2 v'_3 (v'_2 + v'_3)], \quad (41)$$

$$\tilde{v}'_3^{\text{STM}} = \frac{v_3 v'_3}{F_3} (v'_1 + v'_3)(v'_2 + v'_3), \quad (42)$$

$$F_3 = (v'_1 + v'_3)(v'_2 + v'_3)(v_3 + v'_3) + v_3 v'_3 (v'_1 + v'_3) + v_2 v'_3 (v'_2 + v'_3). \quad (43)$$

Now the problem is reduced to the problem of finding of the reversal time of magnetization of a single-atomic chain. However, we cannot use Eq. (29) because the rates of the magnetic moment flipping are different at the different ends of a biatomic chain ($\tilde{v}_1 \neq \tilde{v}_1^{\text{STM}}$, $\tilde{v}_2 \neq \tilde{v}_2^{\text{STM}}$, $\tilde{v}'_3 \neq \tilde{v}'_3^{\text{STM}}$). The derivation of equation for the reversal time of magnetization of a single-atomic chain is similar to our previous calculations [52,53]. Below we discuss only the basic steps of the derivation. If the chain consists of N atoms, then the domain wall can occupy $N + 1$ positions, as it is shown in Fig. 1. The transition rates are equal to

$$v_{0 \rightarrow 1} = \tilde{v}_1^{\text{STM}}, \quad v_{1 \rightarrow 2} = \tilde{v}'_3^{\text{STM}}, \quad v_{N-1 \rightarrow N} = \tilde{v}_2, \quad (44)$$

$$v_{2 \rightarrow 3} = \dots = v_{N-2 \rightarrow N-1} = v_{2 \rightarrow 1} = \dots = v_{N-2 \rightarrow N-3} = \tilde{v}_3, \quad (45)$$

$$v_{1 \rightarrow 0} = \tilde{v}_2^{\text{STM}}, \quad v_{N-1 \rightarrow N-2} = \tilde{v}'_3, \quad v_{N \rightarrow N-1} = \tilde{v}_1. \quad (46)$$

The transition probability matrix is found according to Eq. (4):

$$T = \begin{pmatrix} 0 & 1 - a^{\text{STM}} & 0 & \dots & 0 & 0 & 0 \\ 1 & 0 & 1/2 & \dots & 0 & 0 & 0 \\ 0 & a^{\text{STM}} & 0 & \dots & 0 & 0 & 0 \\ \vdots & \vdots & \vdots & \ddots & \vdots & \vdots & \vdots \\ 0 & 0 & 0 & \dots & 0 & 1/2 & 0 \\ 0 & 0 & 0 & \dots & 1/2 & 0 & a \\ 0 & 0 & 0 & \dots & 0 & 1/2 & 0 \end{pmatrix}, \quad (47)$$

where $a = \tilde{v}'_3 / (\tilde{v}_2 + \tilde{v}'_3)$, $a^{\text{STM}} = \tilde{v}'_3^{\text{STM}} / (\tilde{v}_2^{\text{STM}} + \tilde{v}'_3^{\text{STM}})$. After solving the system of Eqs. (5) with $P_i^{\text{init}} = \delta_{0i}$, the reversal

time of magnetization is found by Eq. (6)

$$\begin{aligned} \tau_{\text{STM}}^{\text{strong}} &= \left(\frac{N-3}{2\tilde{v}_3} + \frac{1}{\tilde{v}'_3{}^{\text{STM}}} \right) \left[N - \frac{2(1-2a)}{1-a} \right] \\ &+ \frac{a}{1-a} \left(\frac{1}{\tilde{v}'_3{}^{\text{STM}}} - \frac{1}{\tilde{v}'_3} \right) + \frac{1}{a^{\text{STM}}\tilde{v}'_1{}^{\text{STM}}} \\ &\times \left[N(1-a^{\text{STM}}) - 2(1-2a^{\text{STM}}) + \frac{a-a^{\text{STM}}}{1-a} \right]. \end{aligned} \quad (48)$$

Note that there is no factor 1/2 in Eq. (48) because it is assumed that the remagnetization always begins under the STM tip. This assumption is true if $\tau_{\text{STM}}^{\text{strong}} \ll \tau^{\text{strong}}$. We should replace N by $N-1$ in Eq. (48) for a biatomic chain of type B.

C. Ferromagnetic chains in the external magnetic field

In this section, we consider the remagnetization of biatomic chains under the external magnetic field \mathbf{B} applied along the easy axis of magnetization \mathbf{e} . We focus on the most physically important case of the ferromagnetic chains ($J, J' > 0$). As it can be seen from Refs. [18,19], a strong-coupling approximation ($J \approx J'$) is more applicable for ferromagnetic chains. Here we consider only this approximation [61].

Following Ref. [52], we assume that the magnetic moments of all of the atoms are directed up at the initial moment of time, and $\mathbf{B} = B\mathbf{e}$, where B run positive and negative values. Instead of eight rates $v_1, v'_1, v''_1, v_2, v'_2, v''_2, v_3, v'_3$ used above, the following 16 rates will be necessary: $v_{1\pm}, v'_{1\pm}, v''_{1\pm}, v_{2\pm}, v'_{2\pm}, v''_{2\pm}, v_{3\pm}, v'_{3\pm}$. Note that if the domain wall is in the position $i = 0$ (see Fig. 1) at the initial moment of time, and all of the magnetic moments are directed up, then the index “+” corresponds to the motion of the domain wall to the right ($i \rightarrow i+1$), and the index “-” corresponds to the motion of the domain wall to the left $i \rightarrow i-1$.

First in a strong-coupling approximation the rates $\tilde{v}_{1\pm}, \tilde{v}_{2\pm}, \tilde{v}_{3\pm}$, and $\tilde{v}'_{3\pm}$ should be calculated. The rates $\tilde{v}_{3\pm}$ which do not depend on the type of a biatomic chain will be calculated further. The domain wall can transit from the initial state 0 to the final states I or II through the transient states 1, 2, 3, and 4 (see Fig. 5). However, now the rates of the motion of the domain wall to the right and to the left are different from each other. Instead of Eqs. (19) and (20) we find

$$v_{0 \rightarrow 1} = v_{0 \rightarrow 3} = v_{3+}, \quad v_{0 \rightarrow 2} = v_{0 \rightarrow 4} = v_{3-}, \quad (49)$$

$$v_{2 \rightarrow 0} = v_{4 \rightarrow 0} = v_{1 \rightarrow \text{I}} = v_{3 \rightarrow \text{I}} = v'_{3+}, \quad (50)$$

$$v_{1 \rightarrow 0} = v_{3 \rightarrow 0} = v_{2 \rightarrow \text{II}} = v_{4 \rightarrow \text{II}} = v'_{3-}. \quad (51)$$

The nonzero elements of the transition probability matrix calculated by Eq. (4) are equal to $T_{01} = T_{03} = 1 - b'$, $T_{02} = T_{04} = b'$, $T_{10} = T_{30} = b/2$, $T_{20} = T_{40} = (1-b)/2$, where $b = v_{3+}/(v_{3+} + v_{3-})$ and $b' = v'_{3+}/(v'_{3+} + v'_{3-})$. After solving the

system of Eqs. (5) with $P^{\text{init}} = \{1, 0, 0, 0, 0\}$, we find

$$\begin{aligned} \tilde{v}_{3+} &= \frac{\tau_1^1 P_1 v_{1 \rightarrow \text{I}} + \tau_3^1 P_3 v_{3 \rightarrow \text{I}}}{\tau_{\text{tot}}} \\ &= \frac{2v_{3+}v'_{3+}}{(v'_{3+} + v'_{3-}) + 2(v_{3+} + v_{3-})}, \end{aligned} \quad (52)$$

$$\begin{aligned} \tilde{v}_{3-} &= \frac{\tau_2^1 P_2 v_{2 \rightarrow \text{II}} + \tau_4^1 P_4 v_{4 \rightarrow \text{II}}}{\tau_{\text{tot}}} \\ &= \frac{2v_{3-}v'_{3-}}{(v'_{3+} + v'_{3-}) + 2(v_{3+} + v_{3-})}. \end{aligned} \quad (53)$$

We note the following. First, if B is replaced by $-B$, then Eq. (52) turns to (53). Second, if $B \rightarrow 0$, then Eqs. (52) and (53) tend to (21).

The rates $\tilde{v}_{1\pm}, \tilde{v}_{2\pm}$, and $\tilde{v}'_{3\pm}$ can be calculated in the same way. For a biatomic chain of type A we find

$$\tilde{v}_{1\pm} = \frac{2v_{1\pm}v'_{1\pm}}{v_{1\pm} + v'_{1\pm} + v'_{2\mp}}, \quad (54)$$

$$\begin{aligned} \tilde{v}_{2\pm} &= \frac{2v_{2\pm}v'_{2\pm}(v'_{3\pm} + v'_{3\mp})}{2v_{3\mp}(v'_{1\mp} + v'_{2\pm}) + (v'_{3\pm} + v'_{3\mp})(2v_{2\pm} + v'_{1\mp} + v'_{2\pm})}, \end{aligned} \quad (55)$$

$$\begin{aligned} \tilde{v}'_{3\pm} &= \frac{2v_{3\pm}v'_{3\pm}(v'_{1\pm} + v'_{2\mp})}{2v_{3\pm}(v'_{1\pm} + v'_{2\mp}) + (v'_{3\pm} + v'_{3\mp})(2v_{2\mp} + v'_{1\pm} + v'_{2\mp})}. \end{aligned} \quad (56)$$

For the biatomic chain of type B we find

$$\begin{aligned} \tilde{v}_{1\pm} &= v''_{1\pm} \left[\frac{v'_{1\pm}v_{3\pm}}{v'_{1\pm} + v'_{3\mp}} + \frac{v_{1\pm}v'_{3\pm}}{v'_{2\mp} + v'_{3\pm}} \right] \left[v_{1\pm} + v''_{1\pm} + v'_{2\mp} + v_{3\pm} \right. \\ &\left. + \frac{v_{3\pm}(v'_{1\pm} - v'_{3\mp})}{v'_{1\pm} + v'_{3\mp}} + \frac{v_{1\pm}(v'_{1\pm} - v'_{2\mp})}{v'_{2\mp} + v'_{3\pm}} \right]^{-1}, \end{aligned} \quad (57)$$

$$\begin{aligned} \tilde{v}_{2\pm} &= v''_{2\pm}(v'_{3\pm} + v'_{3\mp}) \\ &\times \frac{v'_{2\pm}v_{3\pm}(v'_{1\mp} + v'_{3\pm}) + v_{2\pm}v'_{3\pm}(v'_{2\pm} + v'_{3\mp})}{(2v_{3\mp} + v'_{3\pm} + v'_{3\mp})F_{1\mp} + (v'_{3\pm} + v'_{3\mp})F_{2\mp}}, \end{aligned} \quad (58)$$

$$\tilde{v}'_{3\pm} = \frac{2v_{3\pm}v'_{3\pm}F_{1\pm}}{(2v_{3\pm} + v'_{3\pm} + v'_{3\mp})F_{1\pm} + (v'_{3\pm} + v'_{3\mp})F_{2\pm}}, \quad (59)$$

where

$$\begin{aligned} F_{1\pm} &= (v_{1\pm} + v'_{2\mp} + v_{3\pm})(v'_{1\pm} + v'_{3\mp})(v'_{2\mp} + v'_{3\pm}) \\ &- v_{3\pm}v'_{3\mp}(v'_{2\mp} + v'_{3\pm}) - v_{1\pm}v'_{2\mp}(v'_{1\pm} + v'_{3\mp}), \end{aligned} \quad (60)$$

$$\begin{aligned} F_{2\pm} &= (v'_{2\mp} - v'_{3\mp})(v_{3\pm}v_{3\mp} - v_{1\pm}v_{2\mp}) \\ &+ (v_{1\pm} + v'_{2\mp} + v_{3\pm})[v_{3\mp}(v'_{1\pm} + v'_{3\mp}) \\ &+ v_{2\mp}(v'_{2\mp} + v'_{3\pm})] \\ &+ v'_{2\mp}v_{3\mp}(v'_{1\pm} + v'_{3\mp}) + v_{2\mp}v'_{3\mp}(v'_{2\mp} + v'_{3\pm}). \end{aligned} \quad (61)$$

Using the found rates, we calculate the reversal time of magnetization of a biatomic ferromagnetic chain under the external magnetic field. Now the problem is reduced to the estimation of the reversal time of magnetization of the single-

atomic chain shown in Fig. 1. The transition rates are the following:

$$\nu_{0 \rightarrow 1} = \tilde{\nu}_{1+}, \quad \nu_{1 \rightarrow 2} = \tilde{\nu}'_{3+}, \quad \nu_{N-1 \rightarrow N} = \tilde{\nu}_{2+}, \quad (62)$$

$$\nu_{2 \rightarrow 3} = \dots = \nu_{N-2 \rightarrow N-1} = \tilde{\nu}_{3+}, \quad (63)$$

$$\nu_{1 \rightarrow 0} = \tilde{\nu}_{2-}, \quad \nu_{N-1 \rightarrow N-2} = \tilde{\nu}'_{3-}, \quad \nu_{N \rightarrow N-1} = \tilde{\nu}_{1-}, \quad (64)$$

$$\nu_{2 \rightarrow 1} = \dots = \nu_{N-2 \rightarrow N-3} = \tilde{\nu}_{3-}. \quad (65)$$

According to Eq. (4) we find the transition probability matrix

$$T = \begin{pmatrix} 0 & 1 - a'_+ & 0 & \dots & 0 & 0 & 0 \\ 1 & 0 & 1 - b & \dots & 0 & 0 & 0 \\ 0 & a'_+ & 0 & \dots & 0 & 0 & 0 \\ \vdots & \vdots & \vdots & \ddots & \vdots & \vdots & \vdots \\ 0 & 0 & 0 & \dots & 0 & 1 - b & 0 \\ 0 & 0 & 0 & \dots & b & 0 & a'_- \\ 0 & 0 & 0 & \dots & 0 & b & 0 \end{pmatrix}, \quad (66)$$

where $a'_+ = \tilde{\nu}'_{3+}/(\tilde{\nu}_{2-} + \tilde{\nu}'_{3+})$, $a'_- = \tilde{\nu}'_{3-}/(\tilde{\nu}_{2+} + \tilde{\nu}'_{3-})$, and $b = \tilde{\nu}_{3+}/(\tilde{\nu}_{3-} + \tilde{\nu}_{3+})$. After solving the system of Eqs. (5) with $P_i^{\text{init}} = \delta_{0i}$, we find the reversal time of the magnetization by Eq. (6)

$$\begin{aligned} \tau_B^{\text{strong}}(B) = & \frac{1}{2(1-a'_-)} \left\{ \frac{a'_-}{\tilde{\nu}'_{3-}} + \frac{(N-2)(1-a'_-) + (a'_- - \alpha)S_{N-2}}{\tilde{\nu}_{3+}(1-\alpha)} \right. \\ & + \frac{S_{N-2} - (a'_- + \alpha a'_+)S_{N-3} + \alpha a'_+ a'_- S_{N-4}}{\tilde{\nu}_{1+} a'_+} \\ & \left. + \left(\frac{1}{\tilde{\nu}'_{3+}} - \frac{1}{\tilde{\nu}_{3+}} \right) (1-\alpha)[1 - (a'_- - \alpha)S_{N-3}] \right\}, \quad (67) \end{aligned}$$

where $\alpha = (1-b)/b$, $S_N = (1-\alpha^N)/(1-\alpha)$. Equation (67) is valid for biatomic chains of type A. It is necessary to replace N by $N-1$ for chains of type B. Equation (67) has the same structure as Eq. (A5) and tends to Eq. (29) in the limit of $B \rightarrow 0$.

Equation (67) can be used to study the magnetodynamic properties of biatomic chains at the temperatures below T_{max} . If the magnetic field B is a function of time $B = B(t)$, then the rates of remagnetization of biatomic chains $\nu_{\uparrow \rightarrow \downarrow}(t) = 1/\tau_B^{\text{strong}}[B(t)]$ and $\nu_{\downarrow \rightarrow \uparrow}(t) = 1/\tau_B^{\text{strong}}[-B(t)]$ are also functions of time. The probability to find a biatomic chain in the state where the magnetic moments of all of the atoms are directed up can be found from the master equation

$$\frac{dP_{\uparrow}}{dt} = P_{\downarrow} \nu_{\downarrow \rightarrow \uparrow} - P_{\uparrow} \nu_{\uparrow \rightarrow \downarrow}, \quad (68)$$

where $P_{\uparrow} + P_{\downarrow} = 1$ [62]. If the magnetization of a biatomic chain is measured in arbitrary units $M \in [-1, 1]$, then $M = P_{\uparrow} - P_{\downarrow}$. And we find from the master equation (68) the following equation for the magnetization of a biatomic chain:

$$\frac{dM(t)}{dt} = \mathfrak{A}(t)M(t) + \mathfrak{B}(t), \quad (69)$$

where $\mathfrak{A} = -\nu_{\uparrow \rightarrow \downarrow} - \nu_{\downarrow \rightarrow \uparrow}$ and $\mathfrak{B} = \nu_{\downarrow \rightarrow \uparrow} - \nu_{\uparrow \rightarrow \downarrow}$. Equation (69) together with the initial condition $M(0) = M_0$ is the Cauchy problem, which can be easily solved numerically.

D. Numerical estimates

In order to demonstrate the applicability of our method, let us consider the numerical estimates for two physical systems. The first system is the antiferromagnetic Fe chains on Cu₂N/Cu(001) surface. According to the experimental study [30], the exchange energies of Fe atoms are $J = 1.3 \pm 0.1$ meV and $J' = 0.03 \pm 0.02$ meV. In three-atomic chain MAE varies from 2.1 ± 0.1 meV for the edge atoms to 3.6 ± 0.1 meV for the central atom [29]. For the numerical estimates the following parameters of the Hamiltonian $J = 1.3$ meV, $J' = 0.03$ meV, $K = 3$ meV are chosen. Short chains consisting of $2N = 20$ atoms are considered. Note that with this choice of parameters $J/J' \approx 43$ and $J/(NJ') \approx 4.3$. Thus, a weak-coupling approximation should work well. The critical temperature T_C for a single-atomic chain is estimated by the means of the kMC method [43]. We found that T_C decreases monotonically with increasing of the chain length from 10 ± 1 K at $N = 10$ to 6 ± 1 K at $N = 100$. Obviously, the critical temperature of a biatomic chain is higher than T_C of a single-atomic chain. The most of numerical estimations will be performed at the temperature $T = 4$ K. The Fe biatomic chains are definitely in the antiferromagnetic state at this temperature. By varying the parameters of the Hamiltonian (1), the applicability limits of the method will be found.

Figure 10 shows the dependencies of the reversal time of magnetization in the cases of spontaneous remagnetization τ and remagnetization under the interaction with the STM tip τ_{STM} . Solid and dashed lines correspond to a weak and a strong approximation, respectively. The points show the results of the kMC simulations [63]. The upper and the lower plots correspond to the biatomic chains of types A and B, respectively. The estimates of τ^{weak} and $\tau_{\text{STM}}^{\text{weak}}$ are in excellent agreement with the results of the kMC simulation at low exchange energies $J' \ll J$. A weak-coupling approximation works well up to the value of $J' \approx J/N = 0.13$ meV. A strong-coupling approximation works well at $J' \approx J$. Figure 10 shows that a strong-coupling approximation remains valid as J' decreases down to the value of $J/\ln N = 0.56$ meV. Both of the approximations are not very accurate in the intermediate range of $J/N \lesssim J' \lesssim J/\ln N$. However, the function $\min[\tau_{\text{STM}}^{\text{weak}}, \tau_{\text{STM}}^{\text{strong}}]$ can be used as the upper limit of the reversal time of magnetization τ_{STM} . Note that the reversal time of magnetization in the case of spontaneous remagnetization is a monotonically increasing function of J' and it is slightly different for the chains of types A and B. At the same time, the reversal time of magnetization τ_{STM} is a nonmonotonic function. The functions $\tau_{\text{STM}}(J')$ differ significantly from each other, especially at large J' . In the case of a biatomic chain of type B, the dependence $\tau_{\text{STM}}(J')$ has one local minimum. In the case of a biatomic chain of type A, it has two local minima and one local maximum. It is important to note that the function $\min[\tau_{\text{STM}}^{\text{weak}}, \tau_{\text{STM}}^{\text{strong}}]$ qualitatively describes the behavior of the function $\tau_{\text{STM}}(J')$ at all values of J' [64].

The dependence of the reversal times of the magnetization τ and τ_{STM} on the MAE in the range of $K \in [1, 10]$ meV is shown in Fig. 11. The upper plot corresponds to the case of a weak coupling between the atomic chains $J = 1.3$ meV and $J' = 0.03$ meV, and the lower plot corresponds to the case

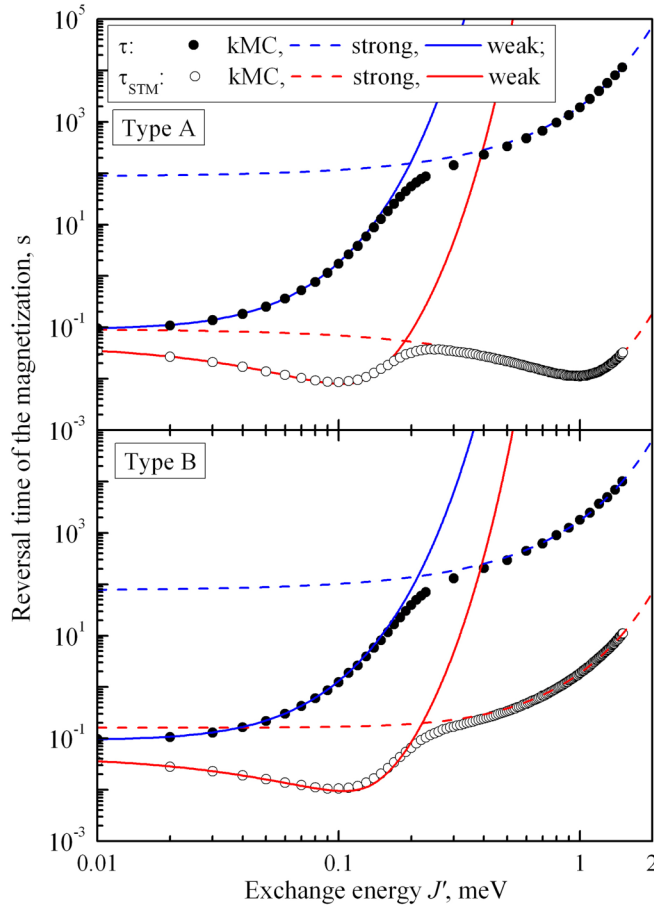


FIG. 10. Dependencies of the reversal time of magnetization on the exchange energy $J' \in [0.01, 1.5]$ meV. The other parameters of the Heisenberg Hamiltonian are the following: $J = 1.3$ meV, $K = 3$ meV, $T = 4$ K, and $2N = 20$. The reversal times of magnetization averaged over 10 000 kMC simulations are shown with points. Solid (dashed) lines correspond to the approximation of a weak (strong) coupling between the chains.

of a strong coupling $J = J' = 1.3$ meV. These dependencies have a very simple form $\ln \tau_{\text{STM}} \sim K$. The reversal times of magnetization of biatomic chains of different types are similar in the case of a weak coupling between atomic chains. But the reversal times of magnetization τ_{STM} differ by three orders of magnitude in the case of a strong coupling between atomic chains. As it can be seen from Fig. 11, the reversal times of magnetization calculated by analytical formulas perfectly agree with the results of the kMC simulations. Note that the conditions of applicability of the single-domain approximation $K(2N) - 2(J + J') \gtrsim k_B T$ (for the chain of type A) and $K(2N) - 2 \max(J, J') \gtrsim k_B T$ (for the chain of type B) are satisfied at $K \geq 1$ meV.

The dependencies of the reversal times of magnetization τ and τ_{STM} on the length of a biatomic chain N are shown in Fig. 12. The total number of atoms in a biatomic chain is $2N$. The upper and the lower plots correspond to the biatomic chains of types A and B, respectively. The results obtained in the framework of a weak-coupling approximation agree well with the results of the kMC simulations at $N < J/J' \approx 43$. With a further increase of N , a weak-coupling approxima-

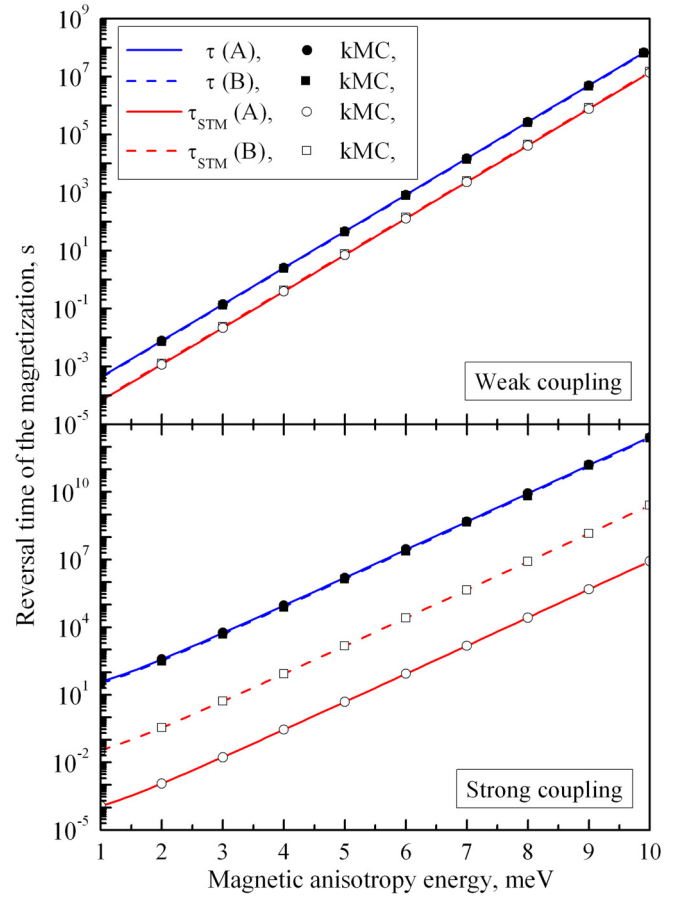


FIG. 11. Dependencies of the reversal time of magnetization on the MAE $K \in [1, 10]$ meV. The other parameters of the Heisenberg Hamiltonian are the following: $J = 1.3$ meV, $J' = 0.03$ meV (upper plot), $J' = 1.3$ meV (lower plot), $T = 4$ K, and $2N = 20$. The reversal times of magnetization averaged over 10 000 kMC simulations are shown with points. Solid and dashed lines correspond to the approximation of a weak (upper plot) and a strong (lower plot) coupling between the chains.

tion leads to a high overestimation of the reversal times of magnetization. Indeed, $\tau_{\text{STM}}^{\text{weak}} \sim e^N$ when $N > J/J'$, while the kMC simulations lead to a linear relationship $\tau_{\text{STM}} \sim N$. A strong-coupling approximation also does not work in this range of the parameters because the condition $J' \ln N \gtrsim J$ is obviously not satisfied. However, $\tau_{\text{STM}}^{\text{strong}} \sim N \sim \tau_{\text{STM}}$. Thus, the estimation $\tau_{\text{STM}}^{\text{strong}}$ can be used as the upper limit on the value of τ_{STM} . For example, the estimate of $\tau_{\text{STM}}^{\text{strong}}$ is in a good agreement with the results of the kMC simulations already at $N \approx 100$ in the case of a biatomic chain of type A.

Let us consider a hypothetical biatomic chain with a strong coupling between atomic chains $J = J' = 1.3$ meV. The dependencies of the reversal times of magnetization τ and τ_{STM} on the length of the chain N are presented in Fig. 13. The dependencies $\tau_{\text{STM}}(N)$ are close to the linear [$\tau_{\text{STM}} \sim N$] for $N \sim 100$. The times τ are almost the same for biatomic chains of types A and B. At the same time, the values of τ_{STM} in the case of chains of type A are several orders lower than those in the case of chains of type B. This is due to the fact that the atom interacting with the STM tip is more

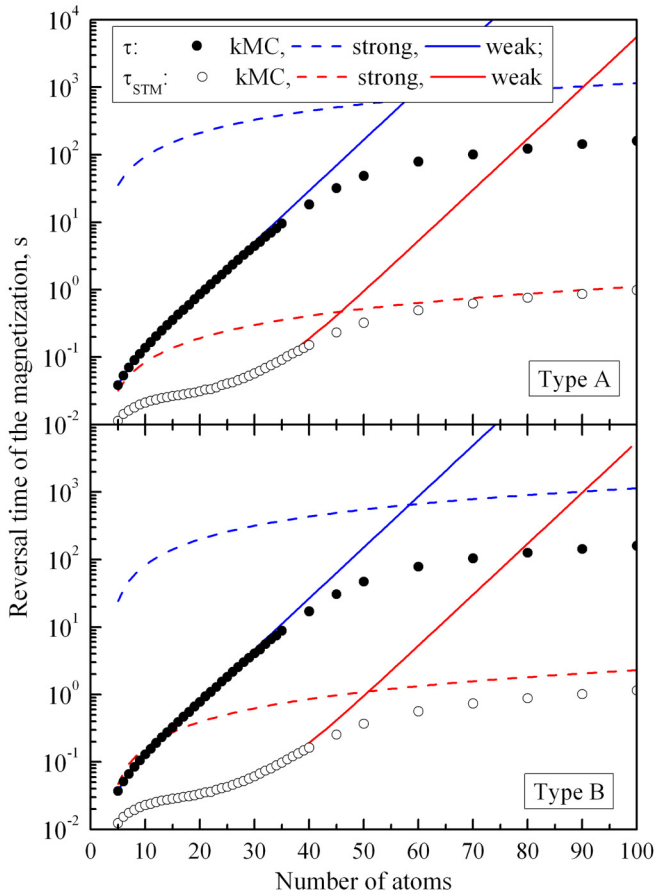


FIG. 12. Dependencies of the reversal time of magnetization on the number of atoms in each of the atomic chains $N \in [5, 100]$. The total number of atoms in a biatomic chain is $2N$. The other parameters of the Heisenberg Hamiltonian are the following: $J = 1.3$ meV, $J' = 0.03$ meV, $K = 3$ meV, and $T = 4$ K. The reversal times of magnetization averaged over 10 000 kMC simulations are shown with points. Solid (dashed) lines correspond to the approximation of a weak (strong) coupling between chains.

strongly coupled with a chain in the case A than in the case B. The reversal times of magnetization calculated in a strong-coupling approximation are in excellent agreement with the results of the kMC simulations.

Figure 14 shows temperature dependence of the reversal times of magnetization τ and τ_{STM} . The upper plot corresponds to a biatomic chain with a weak coupling between the atomic chains $J/J' \approx 43$. The lower plot corresponds to a hypothetical biatomic chain with a strong coupling $J' = J$. We see that in the both cases the values of τ_{STM} calculated by analytical formulas are in excellent agreement with the results of the kMC simulations. Here it is necessary to make two important notes. First, let us discuss the value of the maximum temperature T_{max} till which a single-domain approximation remains valid. The average time of formation of the domain wall τ_+ and the average time of random walk of the domain wall τ_{walk} can be estimated [52]. The temperature T_{max} can be found as a solution of the equation $\tau_+ = \tau_{\text{walk}}$. This equation can be written in the form (A4). However, in the case of short atomic chains $N \leq 100$ the simultaneous appearance of two or more domain walls actually means transition to paramagnetic

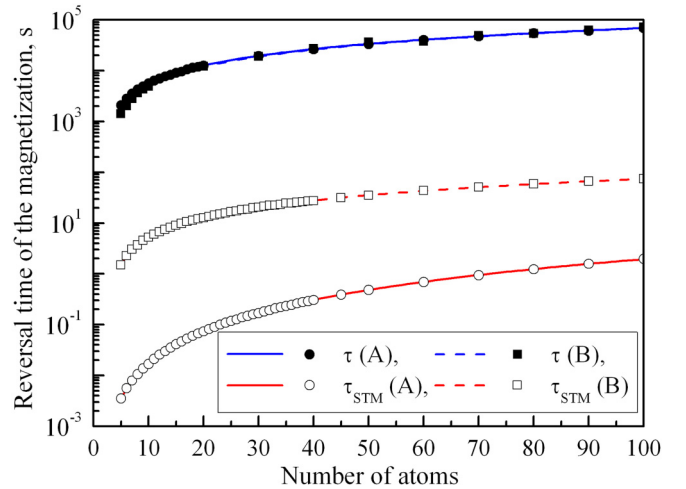


FIG. 13. Dependencies of the reversal time of magnetization on the number of atoms in each of the atomic chains $N \in [5, 100]$. The total number of atoms in the biatomic chain is $2N$. The other parameters of the Heisenberg Hamiltonian are the following: $J = J' = 1.3$ meV, $K = 3$ meV, and $T = 4$ K. The reversal times of the magnetization averaged over 10 000 kMC simulations are shown with points. Solid and dashed lines correspond to the approximation of a strong coupling between the chains.

phase. Thus, the proposed method for estimating of the reversal time of magnetization of biatomic chains leads to adequate results almost up to critical temperature $T_{\text{min}} \approx T_C$. Second, the calculation time needed for the kMC simulations grows exponentially with the decrease of temperature. Therefore, the calculation of the values of τ_{STM} and τ at low temperatures by the means of the kMC method is almost impossible. In this case, the proposed method seems to be the only possible opportunity for estimating of the reversal time of magnetization.

The second system under the consideration is Co biatomic chains on Pt (997) surface. According to Refs [11,19] the exchange energies are $J \approx J' \approx 7.5$ meV, the MAE is $K = 0.33 \pm 0.04$ meV for biatomic Co chain. The magnetic moment of Co atom μ is the sum of the spin magnetic moment $\mu_S \approx 2.08\mu_B$ and the orbital magnetic moment $\mu_L \approx 0.37\mu_B$, where μ_B is the Bohr magneton. For the numerical estimates, we choose the following parameters of the Hamiltonian: $J = J' = 7.5$ meV, $K = 0.34$ meV, and $\mu = 2.4\mu_B$. In order to prevent the simultaneous flipping of magnetic moments of the atoms (the superparamagnetic regime) the following inequalities must be satisfied: $KN - 2J \gtrsim k_B T$ for a single-atomic chain, $K(2N) - 2(J + J') \gtrsim k_B T$ for a biatomic chain of type A, and $K(2N) - 2 \max(J, J') \gtrsim k_B T$ for a biatomic chain of type B. For single-atomic chains at the temperature range of 30–70 K, this condition is satisfied for chains longer than 70 atoms. Further, we consider biatomic chains consisting of $2N = 200$ atoms, which are definitely ferromagnetic. We will see later that the critical temperature of such biatomic chains is approximately 70 K.

Equation (67) for the reversal time of magnetization of a chain τ_B^{strong} under the external magnetic field will not be discussed separately. Instead, we proceed to calculation of magnetization curves $M(B)$. We need to solve Eq. (69) numerically. It is obvious that the obtained magnetization

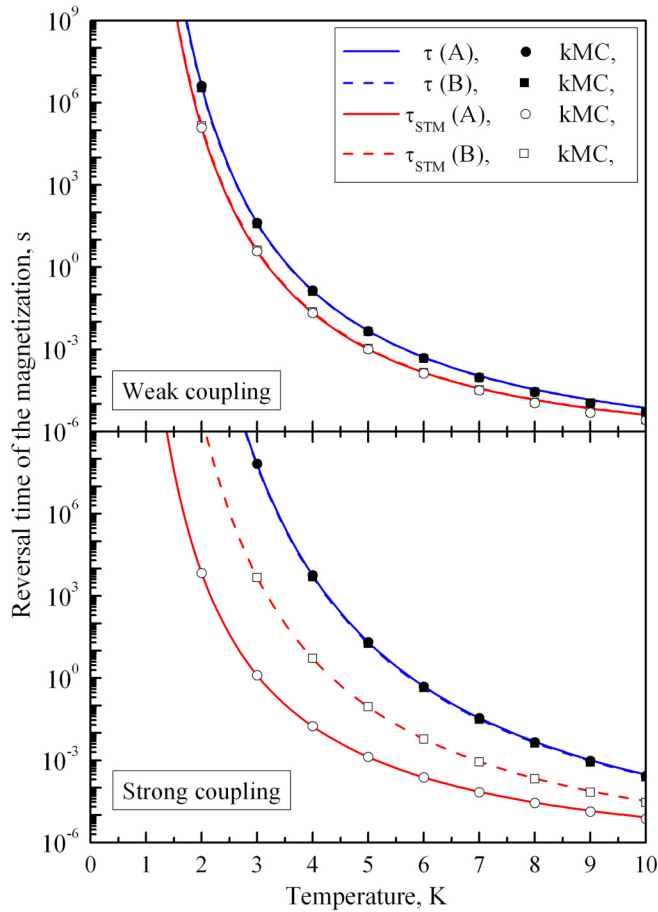


FIG. 14. Dependencies of the reversal time of magnetization on temperature $T \in [0, 10]$ K. The other parameters of the Heisenberg Hamiltonian are the following: $J = 1.3$ meV, $J' = 0.03$ meV (upper plot), $J' = 1.3$ meV (lower plot), $K = 3$ meV, and $2N = 20$. The reversal times of magnetization averaged over 10 000 kMC simulations are shown with points. Solid and dashed lines correspond to the approximation of a weak (upper plot) and strong a (lower plot) coupling between chains.

curves will agree with the results of the kMC simulations only if Eq. (67) gives a correct estimate of τ_B under any external magnetic field B . Following Ref. [45] we start from a strong field $B_0 = -5$ T. The field strength increases by an increment 0.001 T gradually to 5 T. Then the field decreases back to B_0 , so that a sweeping cycle is complete. We consider that the magnitude of the sweeping rate of the external magnetic field $|dB/dt|$ is 130 T/s. The results of the kMC simulations are averaged over 1000 cycles.

Figure 15 shows the magnetization curves of biatomic Co chain of type A at three different temperatures: 40 K, 60 K, and 80 K. If temperature increases from 40 K to 60 K, then the coercive field B_C of the chain drops almost to zero, but the chain remains ferromagnetic. It is clearly seen from the almost constant slope of the hysteresis loop obtained by the means of the kMC method. If the temperature increases to 80 K, then the angle of the slope decreases significantly, which corresponds to the transition of the chain to paramagnetic state. Thus, we can roughly estimate the critical temperature of a biatomic chain as $T_C = 70 \pm 10$ K [65]. The solid

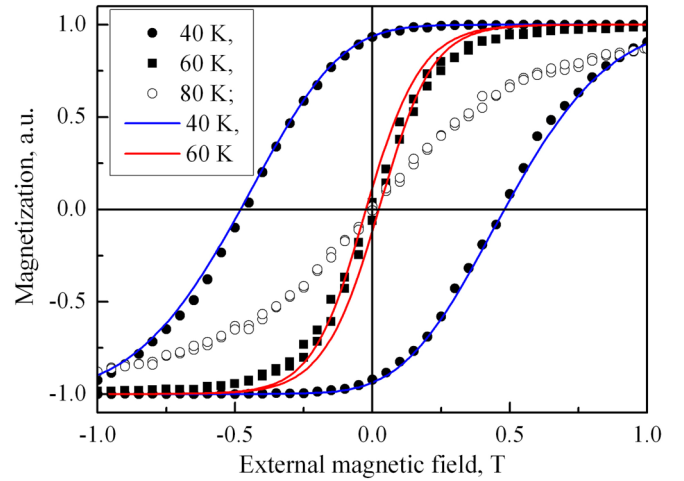


FIG. 15. Magnetization response to the external magnetic field for a biatomic chain of type A consisting of $2N = 200$ atoms at three temperatures: 40 K, 60 K, and 80 K. The parameters of the Heisenberg Hamiltonian are the following: $J = J' = 7.5$ meV, $K = 0.34$ meV, and $\mu = 2.4\mu_B$. Magnetization curves averaged over 1000 cycles of the kMC simulations are shown with points. Solid lines correspond to the solutions of Eq. (69).

curves in Figure 15 show the magnetization curves obtained by solving Eq. (69). We see that the agreement with the results of the kMC simulations is very good at 40 K. But the magnetization curve is slightly different from the results of the kMC simulations at 60 K. In our opinion, such agreement is quite satisfactory. The magnetization curves obtained in the single-domain approximation become more narrow, but do not change their slope with increasing temperature. A single-domain approximation gives inadequate results if the temperature approaches to the critical one.

Figure 16 shows the temperature dependence of the coercive field of a biatomic chain at $T \leq T_C$. The coercive field of biatomic chains of types A and B slightly differ from each other (the difference is less than 10%) because the chains are quite long ($2N = 200$). A single-domain approximation leads to the overestimation of the coercive fields: less than 5% at the temperatures of $T \leq 40$ K, 16% at 50 K, 76% at 60 K, more than twice at $T \geq 65$ K. If the agreement within 20% is considered to be satisfactory, then we can conclude that a single-domain approximation agrees well with the results of the kMC simulations at $T < T_{\max} \approx 0.7T_C$. This conclusion is in good agreement with the estimation of T_{\max} obtained using Eq. (A4) [52].

Let us discuss the applicability limits of a strong-coupling approximation. Figure 17 shows the dependence of the coercive field on the exchange energy J' . The condition of applicability of a strong-coupling approximation remains the same as in the case of $B = 0$ ($J' \gtrsim J/\ln N$) because $\mu_B|B_0| = 0.29$ meV and $\mu_B|B_0| \ll J, J'$. We see that the coercive field obtained in the framework of a strong-coupling approximation differs from the results of the kMC simulations by less than 5% at $J' \geq 4.5$ meV $\approx 2.5J'/\ln N$. If $J' = 2$ meV $\approx J'/\ln N$, then the results differ by about 20%. Thus, we can conclude that a strong-coupling approximation can be used to obtain qualitative results at $J' \gtrsim J/\ln N$, as well as in the absence of

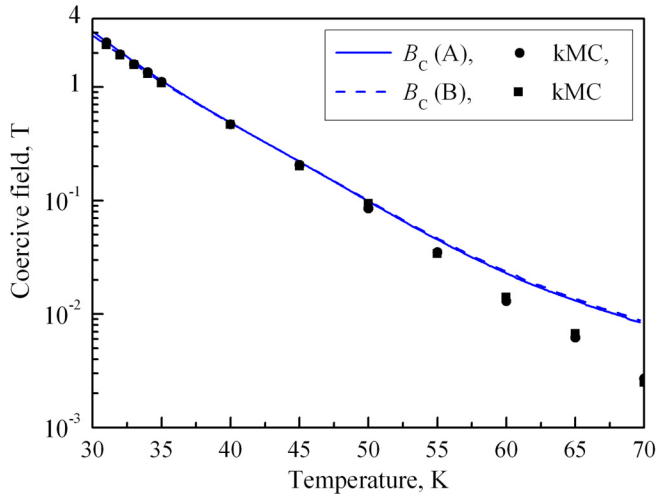


FIG. 16. Temperature dependence of the coercive field B_C for biatomic chains of $2N = 200$ atoms. The parameters of the Heisenberg Hamiltonian are the following: $J = J' = 7.5$ meV, $K = 0.34$ meV, $\mu = 2.4\mu_B$. Results of the kMC simulations averaged over 1000 cycles are shown with points. Solid and dashed lines correspond to the solutions of Eq. (69) for the chains of types A and B, respectively.

an external magnetic field. Note that the estimation obtained in a strong-coupling approximation is the upper limit of the value of the coercive field at any J' .

The MAE of Co atoms on Pt(997) surface varies from 0.13 meV/atom for a monolayer to 2.0 meV for a single adatom [11]. We found that the coercive field of the biatomic chain remains almost constant (1.14 T and 1.11 T for the chains of types A and B, respectively) if the MAE varies in this range. These results are in a good agreement with the kMC simulations. Finally, the size effect in the range of $N \in [60, 200]$ atoms was investigated. We found that the coercive field increases by about 2% with an increase in the

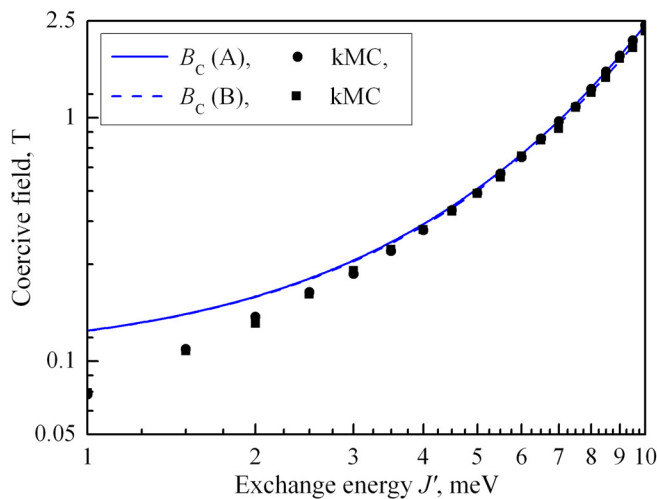


FIG. 17. Dependencies of the coercive field B_C on the exchange energy $J' \in [1, 10]$ meV. The other parameters of the Heisenberg Hamiltonian are the following: $J = 7.5$ meV, $K = 0.34$ meV, $\mu = 2.4\mu_B$, and $2N = 200$. Results of the kMC simulations averaged over 1000 cycles are shown with points. Solid and dashed lines correspond to the solutions of Eq. (69) for chains of types A and B, respectively.

length of a biatomic chain in this range. These results are also in a good agreement with the results of the kMC simulations.

IV. CONCLUSION

We have considered the remagnetization of the biatomic chains in the framework of the Heisenberg model with uniaxial magnetic anisotropy and a single domain-wall approximation. In a general case a calculation of the reversal time of magnetization of biatomic chains is quite a difficult task. Therefore, we considered two limiting cases: a weak and a strong coupling between atomic chains. In the both cases, the problem of remagnetization of biatomic chains is reduced to the problem of remagnetization of single-atomic chains. Equations for estimation the reversal times of magnetization of biatomic chains in three different cases have been derived: (i) the spontaneous remagnetization, (ii) the remagnetization under the interaction with the STM tip, and (iii) the remagnetization under the external magnetic field parallel to the easy axis of magnetization. The first two cases relate to both ferromagnetic and antiferromagnetic chains. The third case relates to ferromagnetic chains. For these chains, we also developed a method for calculation of magnetization curves and the coercive field.

Let us summarize the applicability limits of the method. The thickness of the domain wall can be neglected if $J/2KN^2 \ll 1$. A single domain-wall approximation is valid in a wide range of temperatures from the very low quantum tunneling temperature T_{QT} to the maximal temperature $T_{max} < T_C$. The numerical estimations show that in practically important cases the maximal temperature T_{max} is higher than $0.7T_C$. In order to eliminate the superparamagnetic regime, the following conditions must be satisfied: $K(2N) - 2(J + J') \gtrsim k_B T$ for chains of type A and $K(2N) - 2 \max(J, J') \gtrsim k_B T$ for chains of type B. The approximation of a weak coupling between atomic chains is valid if $J'N \lesssim J$, and a strong-coupling approximation is valid if $J' \ln N \gtrsim J$. In the middle range $J' \ln N \lesssim J \lesssim J'N$, both approximations do not give quantitative agreement with the results of the kMC simulation. However, the function $\min[\tau_{(STM)}^{weak}, \tau_{(STM)}^{strong}]$ can be used in this range both to estimate the upper value of $\tau_{(STM)}$ and for a qualitative explanation of the behavior of the $\tau_{(STM)}(J')$ and $\tau_{(STM)}(N)$ dependencies.

It is necessary to underline that the presented analytical method is incomparably less time-consuming than the usual kMC simulations, especially in the cases of low temperatures or long chains. Therefore, the proposed method can be a useful tool for analyzing of magnetic properties of a wide class of biatomic chains.

ACKNOWLEDGMENTS

The research is carried out using the equipment of the shared research facilities of HPC computing resources at Lomonosov Moscow State University [66].

APPENDIX A: REMAGNETIZATION OF SINGLE-ATOMIC CHAINS

Here we summarize the main results of the previous investigations [52,53]. We use the same notations of the rates as in

the Sec. III. Note that these notations differ from the original ones. If $\mathbf{B} = 0$, then the reversal time of magnetization of ferromagnetic or antiferromagnetic single-atomic chain can be obtained as (see also Fig. 1)

$$\tau = \frac{1}{2a} \left\{ \frac{a}{v_3''} \left(\frac{N-1}{2} \right) \left[N - \frac{2(1-2a)}{1-a} \right] + \frac{1}{v_1''} [N(1-a) - 2(1-2a)] \right\}, \quad (\text{A1})$$

where $a = v_3''/(v_2'' + v_3'')$.

If the first atom of the chain interacts with the STM tip, then the reversal time of magnetization is equal to

$$\tau_{\text{STM}} = \frac{1}{v_3''} \left(\frac{N-1}{2} \right) \left[N - \frac{2(1-2a)}{1-a} \right]. \quad (\text{A2})$$

The values of τ and τ_{STM} are related as follows:

$$\tau = \frac{1}{2} \left\{ \tau_{\text{STM}} + \frac{1}{av_1''} [N(1-a) - 2(1-2a)] \right\}. \quad (\text{A3})$$

The obtained equation is applicable under the conditions: (i) $KN - 2J \gtrsim k_B T$ and (ii) $T < T_{\text{max}}$, where temperature T_{max} can be found from the equation

$$\frac{(v_1'' + v_2'' + v_3'')(v_2'' + v_3'')}{v_1'' v_2''} = \left(\frac{N}{2} - 1 \right)^2. \quad (\text{A4})$$

If $\mathbf{B} \neq 0$, then the reversal time of magnetization of ferromagnetic chain ($J > 0$) is equal to

$$\tau_B(B) = \frac{1}{2(1-a_-)} \times \left[\frac{a_-}{v_{3-}''} + \frac{(N-2)(1-a_-) + (a_- - \alpha)S_{N-2}}{v_{3+}''(1-\alpha)} + \frac{S_{N-2} - (a_- + \alpha a_+)S_{N-3} + \alpha a_+ a_- S_{N-4}}{v_{1+}'' a_+} \right], \quad (\text{A5})$$

where $\alpha = (1-b)/b$, $S_N = (1-\alpha^N)/(1-\alpha)$, $a_+ = v_{3+}''/(v_{2-}'' + v_{3+}'')$, $a_- = v_{3-}''/(v_{2+}'' + v_{3-}'')$, and $b = v_{3+}''/(v_{3-}'' + v_{3+}'')$.

If the MAE K' and the exchange energy J' of the edge atoms are different from K and J of all other atoms, then

$$\tau'_{\text{STM}} = \left[\frac{N-5}{2v_3''} + \frac{b}{1-b} \left(\frac{1}{v_1''} + \frac{1}{v_2''} \right) \right] \left[N - \frac{2c}{1-a'} \right], \quad (\text{A6})$$

$$\tau' = \frac{1}{2} \left\{ \tau'_{\text{STM}} + \frac{1}{a'v_3''} \frac{b}{1-b} [N(1-a') - 2c] \right\}, \quad (\text{A7})$$

where $a' = v_1''/(v_3'' + v_1'')$, $b = v_2''/(v_2'' + v_3'')$, $c = 3 - \frac{1}{b} - 2a'$.

APPENDIX B: ESTIMATION OF THE THICKNESS OF A DOMAIN WALL

Let the atoms placed along the x axis, z axis is the easy axis of magnetization, and $\theta_i = \theta(x_i)$ is the angle between \mathbf{s}_i and the z axis. Then the components of \mathbf{s}_i are $(s_i)_x = 0$, $(s_i)_y = s_i \sin \theta_i$, $(s_i)_z = s_i \cos \theta_i$. For simplicity we consider the case of $\mathbf{B} = 0$. Then the magnetic energy of infinite single-atomic chain is the following:

$$E = - \sum_{i>j} J_{ij} \cos(\theta_i - \theta_j) - K \sum_i \cos^2 \theta_i. \quad (\text{B1})$$

To get a rough estimation of the thickness of the domain wall, the index i should be replaced with a dimensionless variable $\tilde{x} = x_i/a$, where a is the nearest-neighbor distance. Then $\theta_{i+1} \approx \theta_i + [d\theta(\tilde{x})/d\tilde{x}]$. And we can present the energy (B2) in the following form:

$$E[\theta] \approx E_0 + \int_{-\infty}^{\infty} \left[\frac{J}{2} \left(\frac{d\theta}{d\tilde{x}} \right)^2 + K \sin^2 \theta \right] d\tilde{x}, \quad (\text{B2})$$

where $E_0 = \text{const}$. Varying this functional we get the following equation:

$$J \left(\frac{d^2 \theta}{d\tilde{x}^2} \right) - 2K \sin \theta \cos \theta = 0. \quad (\text{B3})$$

The solution of this equation with boundary conditions $\theta(-\infty) = \pi$, $\theta(\infty) = 0$, $(d\theta/d\tilde{x})(\pm\infty) = 0$ is well known [67],

$$\theta = \arccos \left[\tanh \left(\sqrt{\frac{2K}{J}} \tilde{x} \right) \right]. \quad (\text{B4})$$

So the thickness of the domain wall is $\delta N \sim \sqrt{J/2K}$ atoms.

The thickness of the domain wall can be neglected if $\delta N \ll N$. This inequality can be written as $J/2KN^2 \ll 1$. Let us check this inequality for the physical systems discussed in Sec. III D. The first system is antiferromagnetic Fe chains on Cu₂N/Cu(001) surface. The parameters of the Hamiltonian are $J = 1.3$ meV, $K = 3$ meV, and $N = 10$. Thus, $J/2KN^2 \approx 0.002 \ll 1$. The second system is ferromagnetic Co chains on Pt(997) surface. The parameters of the Hamiltonian are $J = 7.5$ meV, $K = 0.34$ meV, and $N = 100$. Thus, $J/2KN^2 \approx 0.001 \ll 1$. We see that in both cases the thickness of the domain wall can be neglected.

- [1] I. Zutic, J. Fabian, and S. Das Sarma, *Rev. Mod. Phys.* **76**, 323 (2004).
 [2] S. Bose, *Phys. Rev. Lett.* **91**, 207901 (2003).
 [3] S. Bose, *Contemp. Phys.* **48**, 13 (2007).
 [4] H. Verma, L. Chotorlishvili, J. Berakdar, and S. K. Mishra, *Eur. Phys. Lett.* **119**, 30001 (2017).
 [5] N. D. Mermin, *Quantum Computer Science: An Introduction* (Cambridge University Press, Cambridge, 2007).

- [6] D. J. Choi, N. Lorente, J. Wiebe, K. von Bergmann, A. F. Otte, and A. J. Heinrich, *Rev. Mod. Phys.* **91**, 041001 (2019).
 [7] D. Sander, *J. Phys.: Condens. Matter* **16**, R603 (2004).
 [8] A. Enders, R. Skomski, and J. Honolka, *J. Phys.: Condens. Matter* **22**, 433001 (2010).
 [9] H. Wang, Y. Yu, Y. Sun, and Q. Chen, *Nano* **06**, 1 (2011).
 [10] J. V. Barth, G. Costantini, and K. Kern, *Nature* **437**, 671 (2005).

- [11] P. Gambardella, A. Dallmeyer, K. Maiti, M. C. Malagoli, W. Eberhardt, K. Kern, and C. Carbone, *Nature* **416**, 301 (2002).
- [12] P. Gambardella, S. Rusponi, M. Veronese, S. S. Dhesi, C. Grazioli, A. Dallmeyer, I. Cabria, R. Zeller, P. H. Dederichs, K. Kern, C. Carbone, and H. Brune, *Science* **300**, 1130 (2003).
- [13] H. Brune and P. Gambardella, *Surf. Sci.* **603**, 1812 (2009).
- [14] J. Bansmann, S. H. Baker, C. Binns, J. A. Blackman, J.-P. Bucher, J. Dorantes-Dávila, V. Dupuis, L. Favre, D. Kechrakos, A. Kleibert, K.-H. Meiwes-Broer, G. M. Pastor, A. Perez, O. Toulemonde, K. N. Trohidou, J. Tuaille, and Y. Xie, *Surf. Sci. Rep.* **56**, 189 (2005).
- [15] T. Balashov, T. Schuh, A. F. Takács, A. Ernst, S. Ostanin, J. Henk, I. Mertig, P. Bruno, T. Miyamachi, S. Suga, and W. Wulfhekel, *Phys. Rev. Lett.* **102**, 257203 (2009).
- [16] J. Shen, J. P. Pierce, E. W. Plummer, and J. Kirshner, *J. Phys.: Condens. Matter* **15**, R1 (2003).
- [17] J. Shen, R. Skomski, M. Klaua, H. Jenniches, S. S. Manoharan, and J. Kirschner, *Phys. Rev. B* **56**, 2340 (1997).
- [18] B. Dupé, J. E. Bickel, Y. Mokrousov, F. Otte, K. von Bergmann, A. Kubetzka, S. Heinze, and R. Wiesendanger, *New J. Phys.* **17**, 023014 (2015).
- [19] P. Gambardella, A. Dallmeyer, K. Maiti, M. C. Malagoli, S. Rusponi, P. Ohresser, W. Eberhardt, C. Carbone, and K. Kern, *Phys. Rev. Lett.* **93**, 077203 (2004).
- [20] F. Otte, P. Ferriani, and S. Heinze, *Phys. Rev. B* **89**, 205426 (2014).
- [21] R. Félix-Medina, J. Dorantes-Dávila, and G. M. Pastor, *New J. Phys.* **4**, 100 (2002).
- [22] M. Martins and W. Wurth, *J. Phys.: Condens. Matter* **28**, 503002 (2016).
- [23] A. L. Klavsyuk, S. V. Kolesnikov, and A. M. Saletsky, *JETP Lett.* **99**, 646 (2014).
- [24] S. Pick, V. S. Stepanyuk, A. L. Klavsyuk, L. Niebergall, W. Hergert, J. Kirschner, and P. Bruno, *Phys. Rev. B* **70**, 224419 (2004).
- [25] O. Gomonay, V. Baltz, A. Brataas, and Y. Tserkovnyak, *Nat. Phys.* **14**, 213 (2018).
- [26] V. Baltz, A. Manchon, M. Tsoi, T. Moriyama, T. Ono, and Y. Tserkovnyak, *Rev. Mod. Phys.* **90**, 015005 (2018).
- [27] E. V. Gomonay and V. M. Loktev, *Low Temp. Phys.* **40**, 17 (2014).
- [28] T. Jungwirth, X. Marti, P. Wadley, and J. Wunderlich, *Nat. Nanotechnol.* **11**, 231 (2016).
- [29] S. Yan, D.-J. Choi, J. A. J. Burgess, S. Rolf-Pissarczyk, and S. Loth, *Nat. Nanotechnol.* **10**, 40 (2015).
- [30] S. Loth, S. Baumann, C. P. Lutz, D. M. Eigler, and A. J. Heinrich, *Science* **335**, 196 (2012).
- [31] M. Etzkorn, C. F. Hirjibehedin, A. Lehnert, S. Ouazi, S. Rusponi, S. Stepanow, P. Gambardella, C. Tieg, P. Thakur, A. I. Lichtenstein, A. B. Shick, S. Loth, A. J. Heinrich, and H. Brune, *Phys. Rev. B* **92**, 184406 (2015).
- [32] A. Ferrón, J. L. Lado, and J. Fernández-Rossier, *Phys. Rev. B* **92**, 174407 (2015).
- [33] D.-J. Choi, R. Robles, J.-P. Gauyacq, M. Ternes, S. Loth, and N. Lorente, *Phys. Rev. B* **94**, 085406 (2016).
- [34] M. C. Urdaniz, M. A. Barral, and A. M. Llois, *Phys. Rev. B* **86**, 245416 (2012).
- [35] K. Tao, Q. Guo, P. Jena, D. Xue, and V. S. Stepanyuk, *Phys. Chem. Chem. Phys.* **17**, 26302 (2015).
- [36] M. C. Urdaniz, M. A. Barral, A. M. Llois, and A. Saúl, *Phys. Rev. B* **90**, 195423 (2014).
- [37] J.-P. Gauyacq, S. M. Yaro, X. Cartoixa, and N. Lorente, *Phys. Rev. Lett.* **110**, 087201 (2013).
- [38] J.-P. Gauyacq and N. Lorente, *J. Phys.: Condens. Matter* **27**, 455301 (2015).
- [39] F. Delgado, S. Loth, M. Zielinski, and J. Fernández-Rossier, *Europhys. Lett.* **109**, 57001 (2015).
- [40] K. Tao, O. P. Polyakov, and V. S. Stepanyuk, *Phys. Rev. B* **93**, 161412(R) (2016).
- [41] H. Ebert, D. Ködderitzsch, and J. Minár, *Rep. Prog. Phys.* **74**, 096501 (2011).
- [42] L. D. Landau and E. Lifshitz, *Phys. Z. Sowjetunion* **8**, 153 (1935).
- [43] Y. Li and B.-G. Liu, *Phys. Rev. B* **73**, 174418 (2006).
- [44] J. Li and B.-G. Liu, *J. Magn. Magn. Mater.* **378**, 186 (2015).
- [45] A. S. Smirnov, N. N. Negulyaev, W. Hergert, A. M. Saletsky, and V. S. Stepanyuk, *New J. Phys.* **11**, 063004 (2009).
- [46] Y. Li and B.-G. Liu, *Phys. Rev. Lett.* **96**, 217201 (2006).
- [47] K. M. Tsysar, S. V. Kolesnikov, and A. M. Saletsky, *Chin. Phys. B* **24**, 097302 (2015).
- [48] S. V. Kolesnikov, K. M. Tsysar, and A. M. Saletsky, *Phys. Solid State* **57**, 1513 (2015).
- [49] K.-C. Zhang and B.-G. Liu, *Phys. Lett. A* **374**, 2058 (2010).
- [50] D. I. Bazhanov, O. V. Stepanyuk, O. V. Farberovich, and V. S. Stepanyuk, *Phys. Rev. B* **93**, 035444 (2016).
- [51] K. M. Tsysar, S. V. Kolesnikov, I. I. Sitnikov, and A. M. Saletsky, *Mod. Phys. Lett. B* **31**, 1750142 (2017).
- [52] S. V. Kolesnikov, *JETP Lett.* **103**, 588 (2016).
- [53] S. V. Kolesnikov and I. N. Kolesnikova, *J. Exp. Theor. Phys.* **125**, 644 (2017).
- [54] It is necessary to distinguish two different processes which may occur in an atomic chain: a propagation of spin waves and a switching of the magnetization. In the current paper a switching of magnetization is considered. A propagation of spin waves is beyond the scope of our research.
- [55] All possible situations are shown in Fig. 1 of Ref. [43].
- [56] R. J. Glauber, *J. Math. Phys.* **4**, 294 (1963).
- [57] This function is discontinuous. Instead of (3) one can use, for example, the expression $v(h_i) = v_0 \min[1, \exp(-2h_i/k_B T)]$. Then the function $v(h_i)$ will be continuous. In any case, it does not affect the applicability limits of our model, because we use the same functions $v(h_i)$ for analytical estimations and the kMC simulations.
- [58] B. Puchala, M. L. Falk, and K. Garikipati, *J. Chem. Phys.* **132**, 134104 (2010).
- [59] M. Athenes, P. Bellon, and G. Martin, *Philos. Mag. A* **76**, 565 (1997).
- [60] The transition probability matrix can be easily diagonalized analytically in one-dimensional or quasi-one-dimensional cases. For two-dimensional or three-dimensional structures the diagonalization can be performed numerically.
- [61] A case of a weak coupling $J' \ll J$ is much simpler. Estimations in this limit can be obtained by generalizing Eqs. (10). Generalization of the equations obtained below to the case of antiferromagnetic chains is also not difficult.
- [62] We assume that the average time of random walk of the domain wall is much less than the average time of the formation of new domain wall. This condition is satisfied if $T < T_{\max}$ [52].

- [63] In this and the following plots, the errors of the kMC simulation results do not exceed the size of the marker.
- [64] We also tried to describe the dependence of $\tau_{(\text{STM})}(J')$ by the function $\{[\tau_{(\text{STM})}^{\text{weak}}]^{-1} + [\tau_{(\text{STM})}^{\text{strong}}]^{-1}\}^{-1}$. Unfortunately, this function is not much better than the function $\min[\tau_{(\text{STM})}^{\text{weak}}, \tau_{(\text{STM})}^{\text{strong}}]$ and also does not lead to quantitative agreement with the results of the kMC simulations in the whole range of parameters.
- [65] The exact determination of the critical temperatures is beyond the scope of this article. Here we only want to demonstrate the adequacy of our model within its applicability limits.
- [66] V. Sadovnichy, A. Tikhonravov, V. Voevodin, and V. Opanasenko, *Contemporary High Performance Computing: From Petascale toward Exascale* (Chapman & Hall/CRC Computational Science, Boca Raton, FL, 2013), p. 283.
- [67] L. D. Landau and E. M. Lifshitz, *Electrodynamics of Continuous Media*, 1st ed. (Pergamon Press, New York, 1960), Vol. 8.